



ÉCOLE POLYTECHNIQUE FÉDÉRALE DE LAUSANNE

SEMESTER PROJECT REPORT

Preliminary Design of a Lunar Reconnaissance Drone

Authors:

Thomas Pfeiffer & Erik Uythoven

Project supervisor:

Dr. David Rodriguez

Responsible professor:

Prof. Jean-Paul Kneib

Abstract

In this report, a preliminary design study of a compact lunar reconnaissance drone module which will assist exploration rovers is presented. It is designed to assist future exploratory rover missions in difficult environments such as PSRs or extreme topographies. Although similar concepts have been validated on Mars by NASA's Ingenuity helicopter, only few such ideas exist for lunar applications. The main challenges of this project lie in the propulsion system to be used, the thermal system of the drone (due to extreme temperatures) and the 3D mapping of the lunar surface using a flash lidar system. These aspects were studied in detail with promising results: For a drone with a weight of 20 kg, 1 kg of green monopropellant is sufficient to cover a distance of at least 1 km before it needs refuelling. In this report, it is assumed that the lightweight flash lidar technology should be developed enough to allow for 10 cm resolution at 50 m flight altitude. This feasibility and initial design study sets a foundation for lunar drones and exploration of the Moon using flying spacecrafts, although many open questions remain to be solved and detailed designs to be performed.

Acknowledgement

We would like to express our sincere gratitude to Dr. David Rodriguez for his excellent guidance and for his supervision of this project. . We would also like to thank Dr. Hiroyuki Koizumi from the University of Tokyo for his precious technical support and feedback on propulsion and thermal systems. Our gratitude is extended to Mustafa Mete from the EPFL Reconfigurable Robotics Lab for his precious advice on Earth-based drones and visual tracking systems. In addition, we would like to thank Dr. Jan Uythoven for the proofreading of this report. Lastly, we would like to thank the EPFL Space Center (eSpace) led by Prof. Jean-Paul Kneib for this great opportunity.

Contents

1 Introduction 1

2 State of the art 1

3 Lunar environment and PSRs 2

3.1 Surface temperature 2

3.2 Dust 3

3.3 Extreme topography 3

3.4 Radiation 3

3.5 Challenge with existing mapping methods 3

4 Mission definition 4

4.1 Mission objectives 4

4.2 Heritage 4

5 Fundamental design questions 5

5.1 Initial research 6

5.2 Initial analysis results and decision mind-map 9

6 Drone design 12

6.1 Decomposition in subsystems 12

6.2 Functional decomposition and solutions 12

6.3 Product tree 14

6.4 Details for the different subsystems 15

6.5 N2 chart 21

7 Drone base design 23

7.1 Product tree 23

7.2 Decomposition in subsystems 24

7.3 Drone base functions 24

8 System Engineering Results 25

8.1 ConOps 25

8.2 Budgets 26

8.3 Requirements 28

8.4 Risk analysis 28

9 Future work, open questions and limitations 32

10 Author's opinion and outlook 32

11 Conclusions and discussion	33
References	35
A Lidar calculations	39
B Propulsion and flight trajectory calculations	39
B.1 Thrusters arrangement	39
B.2 Flight simulation assumptions	39
B.3 Preliminary simulations	40
B.4 Detailed flight simulation	42
B.5 More detailed flight simulation	42
B.6 Propellant tank mass estimation	43
B.7 Pressurant mass and tank mass estimation	43
B.8 Limitations	44
C Thermal analysis	46
C.1 Assumptions	46
C.2 Calculations	46
C.3 Temperature change results	47
C.4 Model limitations	47
D Power calculations	50
E Risk Analysis	50
F Illustrations	53

List of Figures

1	Color code for the choice and effects diagrams.	9
2	Effects of flying into the sunlight.	10
3	Hopping versus hovering advantages.	10
4	Initial analysis results and decision mind-map.	11
5	Product tree of the lunar drone.	14
6	Choices and effects of spacecraft attitude control technologies.	15
7	Top view (left) and side view (right) of the drone with its four thrusters (red). The x-axis is in the main direction of flight. Angles alpha and beta are at 45 degrees.	16
8	Illustration of the propulsion system of the drone. Note that components such as valves, tubes and pressure regulators are not represented.	17
9	Schematic diagram of the drone's propulsion system (based on [33] and [34]).	18
10	Flight proven copper thermal straps by the Space Dynamics Laboratory (SDL) [37].	20
11	N2 chart.	22
12	Product tree of the drone base module.	23
13	Lunar reconnaissance drone module: Concept of Operations. 1. Stand-by mode; 2. Flight preparation and deployment; 3. Vertical ascent; 4. Horizontal flight and surface mapping; 5. Vertical descent and landing.	26
14	Illustration of the drone (Original image: X Energy).	34
B.1	Possible thrusters arrangements: a) One single thruster with reaction wheels / control moment gyroscopes b) 3-4 thrusters on the bottom c) 3-4 lateral thrusters d) One single thruster on gimbal e) One single thruster and 3-4 small lateral thrusters.	40
B.2	Three different flight profiles analyzed.	42
B.3	Drone mass decrease due to propellant consumption.	43
B.4	Detailed flight profile simulation in Simulink.	45
C.1	Drone temperature change ΔT [K] for various elapsed times t with respect to the thermal source power \dot{Q}_{gen} and the emissivity/absorbitivity $\epsilon = \alpha$	48
C.2	Evolution of the drone temperature T with respect to time t for $\dot{Q}_{gen} = 500$ W and $\epsilon = \alpha = 0.8$	48
C.3	Drone equilibrium temperature T_{∞} with respect to the thermal source power \dot{Q}_{gen} and the emissivity/absorbitivity $\epsilon = \alpha$	49
C.4	Drop of the drone temperature T with respect to time t , when the thermal source power is zero.	49
D.1	MP 144350 xlr Rechargeable Li-ion cell by Saft [35].	53
F.1	CAD render of the lunar reconnaissance drone.	53
F.2	Illustration of the drone (Original image: NASA).	54
F.3	Illustration of the drone (Original image: NASA).	54

List of Tables

- 1 Advantages and disadvantages of various mapping sensors 6
- 2 Advantages and disadvantages of various propulsion technologies [23] 7
- 3 Morphological matrix of functions and solutions (selected one in green) 13
- 4 Thruster main specifications [30] 16
- 5 Typical operational and survival temperature ranges of various components according to Larson et al [31], adapted and extended by the authors 19
- 6 Preliminary mass budget 27
- 7 Preliminary power budget 27
- 8 Severity matrix and risk color code 28
- 9 Preliminary drone requirements 30
- 10 Preliminary drone base requirements 31
- B.1 Thruster arrangement advantages and disadvantages 41
- B.2 Results of preliminary trajectory calculations 41
- B.3 Results of the more detailed simulation 42
- B.4 Pressurant comparison 44
- D.1 MP 144350 xlr Rechargeable Li-ion cell specifications [35] 50
- E.1 Preliminary risk analysis 51

Acronyms

AGL Above Ground Level. 6, 33

AV Avionics. 12

CDH Communication and data handling. 5, 12, 24

CMG Control Moment Gyroscopes. 39

ConOps Concept of Operations. 25, 32–34

DoD Depth-of-Discharge. 50

EL3 European Large Logistics Lander. 4, 5, 18, 33

EPFL École polytechnique fédérale de Lausanne. 1, 28

ERT EPFL Rocket Team. 28

ESA European Space Agency. 4, 5, 18

eSpace EPFL Space Center. ii

FMEA Failure Mode and Effects Analysis. 28, 50

FoS Factor of Safety. 43, 44

GPIM Green Propellant Infusion Mission. 17

HPGP High Performance Green Propulsion. 16

IF Interfaces. 24

IMU Inertial Measurement Unit. 20

JPL Jet Propulsion Laboratory. 1

Lidar laser imaging, detection, and ranging. 4, 6, 7, 13, 18, 21, 25, 27–29, 33, 39

LRO Lunar Reconnaissance Orbiter. 3, 4

MIT Massachusetts Institute of Technology. 2

NASA National Aeronautics and Space Administration. 1, 2, 4, 5, 17

OBC On-Board Computer. 21

PL Payload. 12

PR Propulsion. 12, 24

PSR Permanently Shadowed Regions. 1–4, 7–9, 19, 21, 33, 34

PWR Power. 12, 24

RCS Reaction Control System. 13

RW Reaction Wheels. 39

ST Structures. 12, 24

TH Thermal. 12, 24

UAVs unmanned aerial vehicles. 20

VIPER Volatiles Investigating Polar Exploration Rover. 4

WEB Warm Electronics Box. 17, 19

1 Introduction

For over 50 years our Moon has been the primary target of human exploration in space. However, only twelve astronauts have visited its surface so far [1] and Mars is moving more and more into the spotlight. Nevertheless, the Moon still is of great scientific interest to space agencies, not least as a test and preparation for visiting Mars. With the Artemis mission, the National Aeronautics and Space Administration (NASA) is preparing to bring humans back to the Moon for the first time after several decades [2]. Moon bases are planned to be built and therefore lunar exploration is one of the challenges to be mastered in the future. In the search of possible locations for lunar bases the lunar South Pole is of particular interest as water ice is expected to be found in these regions [3, 4, 5]. However, these regions represent significant challenges for exploration to most wheeled rovers designed so far. The extremely low temperatures due to everlasting shadows in these so called Permanently Shadowed Regions (PSR) and the lack of sunlight are the main reasons for these difficulties.

Until now, mostly wheeled rovers are used for uncrewed exploration of extraterrestrial and lunar surfaces. However, they are often large and bulky due to the complex payload they carry (power, scientific instruments, communication, etc.) and are limited in terms of locomotion, especially in difficult terrain. Precise knowledge about their environment for route planning is crucial and often rely on limited-resolution satellite data from lunar orbiters, which is even worse in PSRs. The need of a simple, lightweight and cheap scouting method is becoming more and more apparent. Unlike on Mars, which has an atmosphere allowing for drones with propellers such as the Ingenuity helicopter [6] to fly, the Moon does not have any atmosphere and alternative solutions are required.

The goal of this project is to study the feasibility of a compact lunar reconnaissance drone module for rovers and to propose a preliminary design. It highlights the main challenges of such a system and sets the baseline for future developments.

The study is realized as a semester project by two Master students at the École polytechnique fédérale de Lausanne (EPFL), both with a background in Mechanical Engineering. The project started in September of 2021 and ended in January of 2022.

2 State of the art

The use of lightweight and compact vehicles for exploration of unknown terrain is not new and has evolved especially in the last decades with the miniaturization of electrical and mechanical components: On Earth, drones are being used to explore disaster and war zones before sending in humans. In addition, they are used for repetitive tasks such as surveillance for wildfire prevention or inspection of buildings and factories. They have the advantage of easy and fast deployment and operation, all while being cheap and transportable. Outside Earth, the Ingenuity helicopter by NASA's Jet Propulsion Laboratory (JPL) is the first powered controlled extraterrestrial aircraft successfully tested on the martian surface [6]. On the Moon however, no such vehicles exist yet and have only been proposed in a few concept studies so far.

In a Master's thesis from 2011 on the development of a cold gas propulsion system for the TALARIS Hopper [7] written at the Massachusetts Institute of Technology (MIT), a lunar hopper prototype for Earth-based testing equipped with a cold gas propulsion system is proposed. The thesis focuses on the propulsion system of the hopper and its testing and represents a great base for the development of future lunar hoppers. In a thesis from 2013 ("Mission Design for Safe Traverse of Planetary Hoppers") by B.E. Cohanin [8], a detailed study of planetary hoppers for exploration purposes is presented. A group of Master students from the University of Southampton have successfully designed and tested a prototype of a "vertical take-off, vertical landing" lunar hopper [9].

In a more recent Master's thesis from 2020 by G. Podestà ("Lunar Nano Drone for a mission of exploration of lava tubes on the Moon: Propulsion System" [10]) another concept of a lunar exploration drone is proposed. It concludes however that with the restrictive 12U constraint imposed on the volume and currently available components this project is not feasible as by now. Nevertheless, it offers another valuable contribution to the research and development of a lunar drone.

Intuitive Machines is an American start-up company planning to send their lunar lander ("Nova-C") together with a lunar hopper/drone called "Micro-Nova" [11]. The goal of this hopper is to explore craters, PSRs and lava tubes on the Moon, especially at its South Pole. As of 2021, Intuitive Machines and NASA have finalized a \$41.6 million dollars contract to built this system [12, 13]. Besides the size of around 80 cm in length, width and height, not many details are known about the Micro-Nova drone.

3 Lunar environment and PSRs

The lunar surface represents a challenging environment for exploration, especially for wheeled rovers. The lunar gravity and the lunar vacuum are two of several constraining factors to be considered. Gravity on the Moon is about 1/6 of Earth's gravity, and the lack of an atmosphere result in an omnipresent hard vacuum and little thermal insulation: Mean surface temperatures range from -155°C during the lunar night to +110°C during the day. The lunar South Pole in particular is even more challenging than for example the landing sites of the Apollo missions, if not the most challenging regions besides lunar lava tubes: So called Permanently Shadowed Regions (PSR)s and extreme topography make exploration by rover very difficult. The most important and restricting aspects of the lunar South Pole are the surface temperature, the dust, the extreme topography and the radiation and are discussed below.

3.1 Surface temperature

With an albedo of 0.07 to 0.10 the Moon absorbs most of the energy coming from the Sun. In combination with the lack of atmosphere, it heats up and cools downs much faster than it is the case on Earth. For these reasons, great temperature differences exist between illuminated surfaces and shadow areas. According to NASA [14], temperatures at the lunar poles vary from 230 K at daytime to 40 K in dark polar craters, the latter often referred to as PSRs.

These regions are never touched by sunlight due to the low angle of incidence and are expected to hold significant amounts of water ice and other volatiles [5, 15].

The extreme gradient in temperature needs to be considered when designing the drone, as thermal expansion and contraction of materials can appear and affect the performance of the system. This temperature gradient does not only appear when contact between drone and any lunar surface is established, but also already between the illuminated side and the dark side of the drone. This is a common problem when designing any spacecraft exposed to the sun and can be solved with smart thermal control and heat distribution.

3.2 Dust

The lunar soil is covered by layers of dust and rock fragments, called regolith. Its density can vary depending on the geographical location but is usually considered sufficient to support larger spacecrafts. The dust adheres to most of the equipment used on the lunar surface. All the components must therefore be sealed. The dust also limits the use of lubricants and renders the use of optical instruments such as camera lenses or mirrors more challenging. Moreover, solar panels are expected to show lower efficiency once coated in the dust [14].

Dust dispersion by the propulsion system of the drone can therefore pose a significant problem not only to the drone itself, but also to the rover or a lunar base it might be deployed from.

3.3 Extreme topography

Lunar topography, especially at the poles, is characterized by rocks, steep craters and several mountain massifs. The latter can have elevation differences of over 8 km depending on the region and stretch out over several tens of kilometers [16, 17]. For a rover on an exploration mission however, minor obstacles such as small rocks or pits in the regolith can become already major issues if not foreseen. Slopes above 20 degrees inclination in combination with these obstacles are challenges not easy to overcome.

3.4 Radiation

Radiation of various types (electromagnetic and particle radiation, ionizing radiation such as solar wind or cosmic rays) and micrometeorites are factors which can have a negative impact on electronics, solar panels and instruments. Proper shielding and radiation-hardened components are aspects to consider in the design of the system [14].

3.5 Challenge with existing mapping methods

Currently, mappings of the moon are done by lunar orbiters, such as the Lunar Reconnaissance Orbiter (LRO). This orbiter provides the highest resolution map of the moon with precision of 0.5 meters per pixel in illuminated regions [18]. In PSRs however, due to the absence of light, the exposure time

of the LRO's cameras needs to be longer. In combination with the orbital velocity, this greatly reduces the mapping precision. Therefore, the most detailed maps inside PSRs made from orbit have a limited resolution of 10 to 20 m/pixel [19]. This is not sufficient to plan rover navigation paths.

4 Mission definition

The semester project's study will be based on two space missions currently being planned: NASA's Volatiles Investigating Polar Exploration Rover (VIPER) mission [20], expected to explore the lunar South Pole in 2023, and ESA's European Large Logistics Lander (EL3) Polar Explorer scientific mission [21, 22], which will take place in the late 2020s and early 2030s. These two missions will explore the polar regions of our Moon, searching for water ice among others. They will encounter two central challenges: Extreme topography and Permanently Shadowed Regions. These two factors present high risks and difficulties to rover navigation.

A lunar reconnaissance drones could provide a solution to these challenges by scouting the path of the rover in advance. Existing concepts however are of significant mass and complexity so far. The mission statement of this study is:

Assist a lunar rover mission in PSRs or extreme topography with a compact lunar reconnaissance drone module.

4.1 Mission objectives

From the mission definition the following objectives of this study are defined:

- Propose a conceptual design of a lightweight and compact lunar drone module for scouting and exploration (localized high resolution mapping) purposes to assist a large-scale lunar rover mission in inaccessible or extreme environments
- Lay a foundation for quick and simple means of exploration for future Moon missions.
- If possible, the drone should be reusable, modular and adaptable.

In this context, high resolution mapping is defined as a mapping of resolution smaller or equal to the characteristic length of a rover. This could for example be the radius of the rover wheel, a few tens of centimeters.

4.2 Heritage

As mentioned before, no existing heritage missions exist so far. However, this project is heavily inspired by reconnaissance drones used on Earth which are usually equipped with optical or infrared cameras. Recently, laser imaging, detection, and ranging (Lidar) systems have often been added as mapping sensor for reconnaissance drones. As for the propulsion system, small satellites such as micro satellites are used as reference. They are relatively well developed and require similar levels of thrust [23].

5 Fundamental design questions

Based on the mission definition stated in [section 4](#), several high level requirements and mission design aspects can be derived. These objectives are based on NASA's Viper mission [\[20\]](#) and ESA's EL3 Lunar Polar Explorer Mission [\[22\]](#). They are listed here:

1. The payload is a high resolution mapping sensor (mission def.).
2. The drone can be deployed multiple times (mission def.).
3. The distance travelled into a PSR by the rover is 250 m (EL3).
4. Day/night cycles:
 - (a) Lunar night of up to 4 Earth days in standby mode (VIPER).
 - (b) 0.25 day/night duty cycle (EL3).
5. The rover mission duration is at least 24 months (EL3) [\[24\]](#).

Designing a mission around these objectives is a central aspect of this project. The main open questions at this point are:

1. Flight strategy:
 - (a) Covered distance.
 - (b) Altitude profile: ballistic hopping with or without landing, flight at constant height, or a combination of both.
 - (c) Trajectory: straight line forth and back, loop circuit, adaptation to the environment, etc.
2. Propulsion system to be used:
 - (a) Propellant type.
 - (b) Thruster configuration.
3. Definition of thermal requirements and identification of technological difficulties.
4. Choice of mapping sensor type.
5. Choice of the power source.
6. Communication and data handling (CDH) strategy.
7. How to manage reusability.
8. Definition of the interfaces with the rover.

5.1 Initial research

Initially, the research is focused on the flight trajectory, propulsion system, thermal analysis and choice of mapping sensor. These are the mission defining choices that need to be done and that are covered below.

5.1.1 Choice of mapping sensor

Four mapping technologies are considered. Their advantages and disadvantages are given in [Table 1](#). Due to these properties, using a flash Lidar seems to be the best option for the lunar reconnaissance drone. A flash Lidar uses a diverging laser beam to illuminate the surface to be scanned in single flashes. The time of flight of the light is measured with a sensor array and a momentary 3D map created from the data. This can be useful for landing maneuvers of spacecraft for example. In contrast, a normal scanning Lidar uses a single-point laser to create a map point-by-point, requiring moving parts in the system [25]. Currently, light weight flash Lidars for space applications are in development and should become available in the near future [26]. These new Lidars are expected to weigh below 4 kg [27, 28, 29].

Table 1: Advantages and disadvantages of various mapping sensors

Sensor type	Advantage	Disadvantage
Visual	<ul style="list-style-type: none">• High resolution	<ul style="list-style-type: none">• Requires extra lighting• High power consumption (due to additional lighting)
Radar	<ul style="list-style-type: none">• Large sensing range	<ul style="list-style-type: none">• Low resolution
Flash Lidar	<ul style="list-style-type: none">• High resolution• Fast	<ul style="list-style-type: none">• Heavy equipment• Limited sensing range
Rotating/scanning Lidar	<ul style="list-style-type: none">• High resolution	<ul style="list-style-type: none">• Moving parts
Thermal	<ul style="list-style-type: none">• Temperature measurement	<ul style="list-style-type: none">• Low resolution due to small thermal variations in PSRs

This choice of mapping sensor also implies certain flight characteristics of the lunar reconnaissance drone. First, the drone shall fly at a constant altitude of around 50 m Above Ground Level (AGL). Secondly, it shall fly at a maximum speed of around 30 m/s (see [Appendix A](#)). These two requirements mainly influence the propulsion system and are acceptable considering the initial research presented in [subsubsection 5.1.2](#).

5.1.2 Propulsion system

The type of propulsion is limited because its thrust level has to be throttleable somewhere between 10 and 100 N. The different considered propulsion technologies with their advantages and disadvantages are given in [Table 2](#). Due to these properties and by looking at existing technologies, the mono-propellant and cold gas systems are kept for further analysis.

Table 2: Advantages and disadvantages of various propulsion technologies [\[23\]](#)

Propulsion type	Advantage	Disadvantage
Mechanical (spring based)	<ul style="list-style-type: none"> No fuel required Can be combined with other propulsion type 	<ul style="list-style-type: none"> Ballistic hops Contact with lunar surface No constant height flight
Cold gas	<ul style="list-style-type: none"> Very simple system No heat generation 	<ul style="list-style-type: none"> Low specific impulse N₂ tanks are large and heavy Throttle by pulsing (often)
Mono-propellant (with catalyzer)	<ul style="list-style-type: none"> Simple system Good specific impulse 	<ul style="list-style-type: none"> Generates heat 2 tanks required (often)
Bi-propellant	<ul style="list-style-type: none"> Very good specific impulse 	<ul style="list-style-type: none"> Very complexe and heavy
Hybrid	<ul style="list-style-type: none"> Simple system Good specific impulse 	<ul style="list-style-type: none"> No refueling possibility Generates heat 2 tanks required (often)
Electric	<ul style="list-style-type: none"> Excellent specific impulse 	<ul style="list-style-type: none"> No sufficient thrust level High electrical energy consumption

Propellant consumption analyzes are performed on various flight trajectories such as ballistic hops, constant height flights or a combination of both. The baseline for these flight profiles is set at around 1000 m of total horizontal distance (enough to map 250 m into a PSR), a horizontal velocity of 30 m/s and a flight height with an average of 50 m due to the flash Lidar mapping sensor (as mentioned in [subsubsection 5.1.1](#)). The propellant mass required for these flights ranges from 90 g to 150 g according to initial calculations depending on the efficiency of the propulsion system, the time of flight and the flight trajectory. For the final drone design with a limited horizontal flight velocity, the propellant mass is increased to around 1 kg, which is still relatively low with respect to the rest of the drone's mass. The details of the calculations are given in [Appendix B](#).

These results imply that the main criteria for the choice of propulsion technology should be the

weight of the entire subsystem, as well as its controllability (throttleability). The type of flight trajectory is not critical from a propulsion point of view. Therefore, the simplest flight strategy should be chosen (see [subsection 5.1.4](#)).

5.1.3 Thermal analysis

The operating temperature of the drone is limited due to the electronic components, propellant tanks, and due to the thermal expansion of optics making the measurements less accurate. Therefore, it is necessary to control the temperature change, especially in the very harsh environment of the Moon. The temperature of the drone should stay between 0 and 50 °C (see [Table 5](#)).

The temperature evolution calculations with respect to time in different scenarios are shown in [Appendix C](#). These show that without adding radiators (added weight and complexity), the heating of the drone should be limited to $\dot{Q}_{gen} = 1500$ W. This heat source is the combination of joule heating, thrusters firing and the incoming sunlight. The surface coating of the drone can be chosen to have an appropriate emissivity and limit the temperature change during the flight. A high emissivity ($\epsilon \geq 0.8$) is required for large heat source powers for flight lasting around 10 minutes ($t = 600$ s). The detailed graphs of the temperature changes can be seen on [Figure C.1](#) and [Figure C.2](#).

If the drone is to be used in the sunlight and in PSRs, the heat source would vary a lot due to the sunlight. Therefore, an active thermal control would be necessary: Either electric heaters would be needed during missions inside PSRs, or radiators would be required for flights in the sunlight. Each comes with advantages and disadvantages and a combination of both would also be possible.

An other way to get rid of heat would be by conduction with the lunar soil. This would however mean that the drone needs to perform a landing on unknown terrain, and that a lot of lunar dust would be dispersed. Therefore, this option is not considered.

Additionally, since the drone will probably have a high emissivity, it will rapidly cool down when it is not used. A graph of this temperature evolution can be seen in [Figure C.4](#). This implies that the drone shall be protected under an insulating heat shield when stored on the rover. It will also have to be connected to the rover's thermal system or have its own heaters to maintain a temperature around 0 °C.

However, it is to be noted that these thermal calculation assume a uniform temperature distribution and constant boundary conditions (no transition between sunlight and shadow is considered). Therefore, a more in depth thermal analysis will be required to further develop the drone and its base.

5.1.4 Flight trajectory

The flight trajectory presents many options which all have different effects, advantages and disadvantages. The options of the study are whether the drone flies into the sunlight or not and whether it performs hops or flies at a constant height. Diagrams with these questions, choices, effects are presented below ([Figure 2](#), [3](#) and [6](#)). They use the color code shown in [Figure 1](#).

One initial choice that has to be made is the role of the sun during the flight. The effects of this

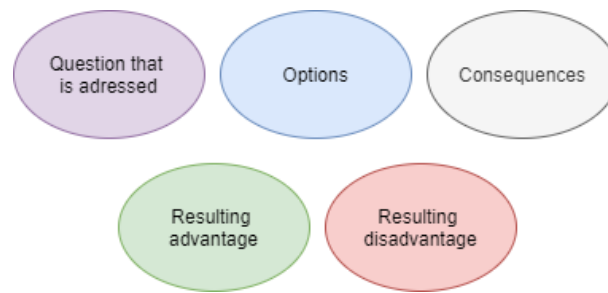


Figure 1: Color code for the choice and effects diagrams.

decision are shown in [Figure 2](#). It can be seen that there are mostly disadvantages of the drone requiring sunlight to function properly due to power and thermal requirements. Moreover, in the later design, it will be shown that solar panels are not necessary if the drone can charge its batteries on the rover (drone base). Therefore, the choice to not go into the sunlight is made.

If a flight into the sunlight is required for other types of missions than exploring PSRs, the thermal systems of the drone will have to evacuate the extra heat, probably by using radiators. This aspect wasn't studied in detail and will depend on the required flexibility of the drone.

Knowing that fuel is no the driving factor of the drone's mass, both ballistic hopping and flying at a constant height need to be considered. Their respective advantages are shown in [Figure 3](#). This figure also includes the scenario of the drone always landing on its base on the rover. This flight strategy has many advantages in terms of reusability (charging and refueling), communication (mapping data can be transferred by wire after landing) and for the flexibility of deployment (drone can be on standby for a long time). It is therefor decided to go with this last strategy: a flight at constant height for mapping with a return to base. This also prevents the drone from landing on the lunar ground and dispersing dust.

5.2 Initial analysis results and decision mind-map

All the results and subsequent decisions are summarized in the decision mind-map shown in [Figure 4](#).

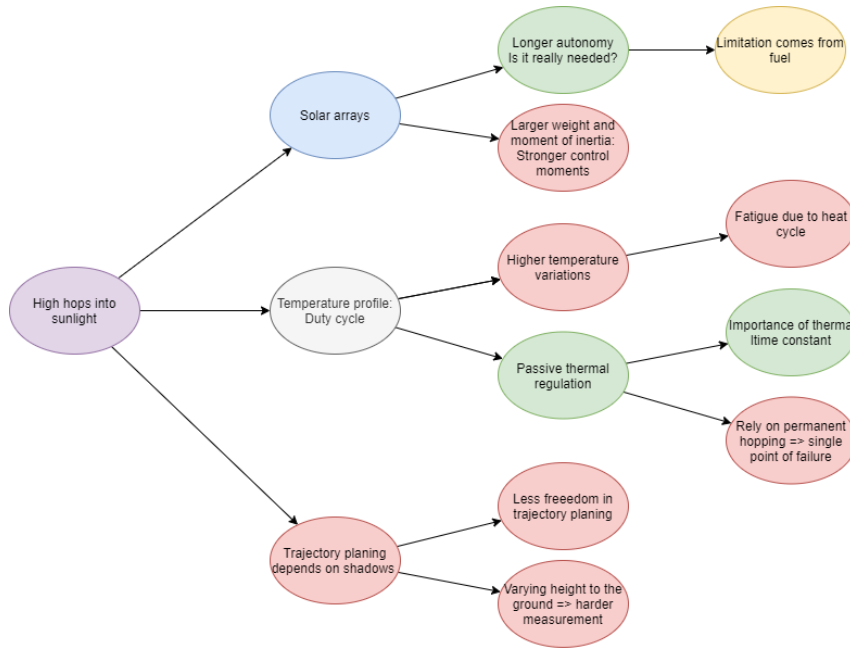


Figure 2: Effects of flying into the sunlight.

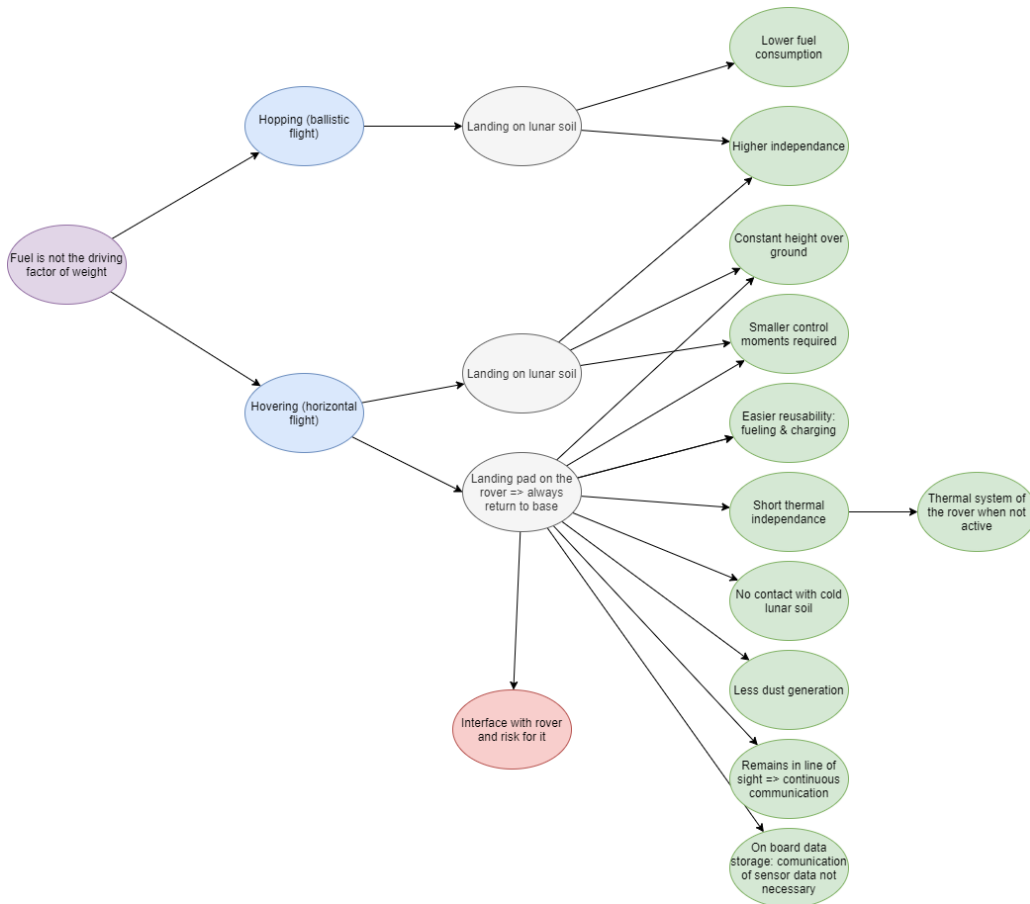


Figure 3: Hopping versus hovering advantages.

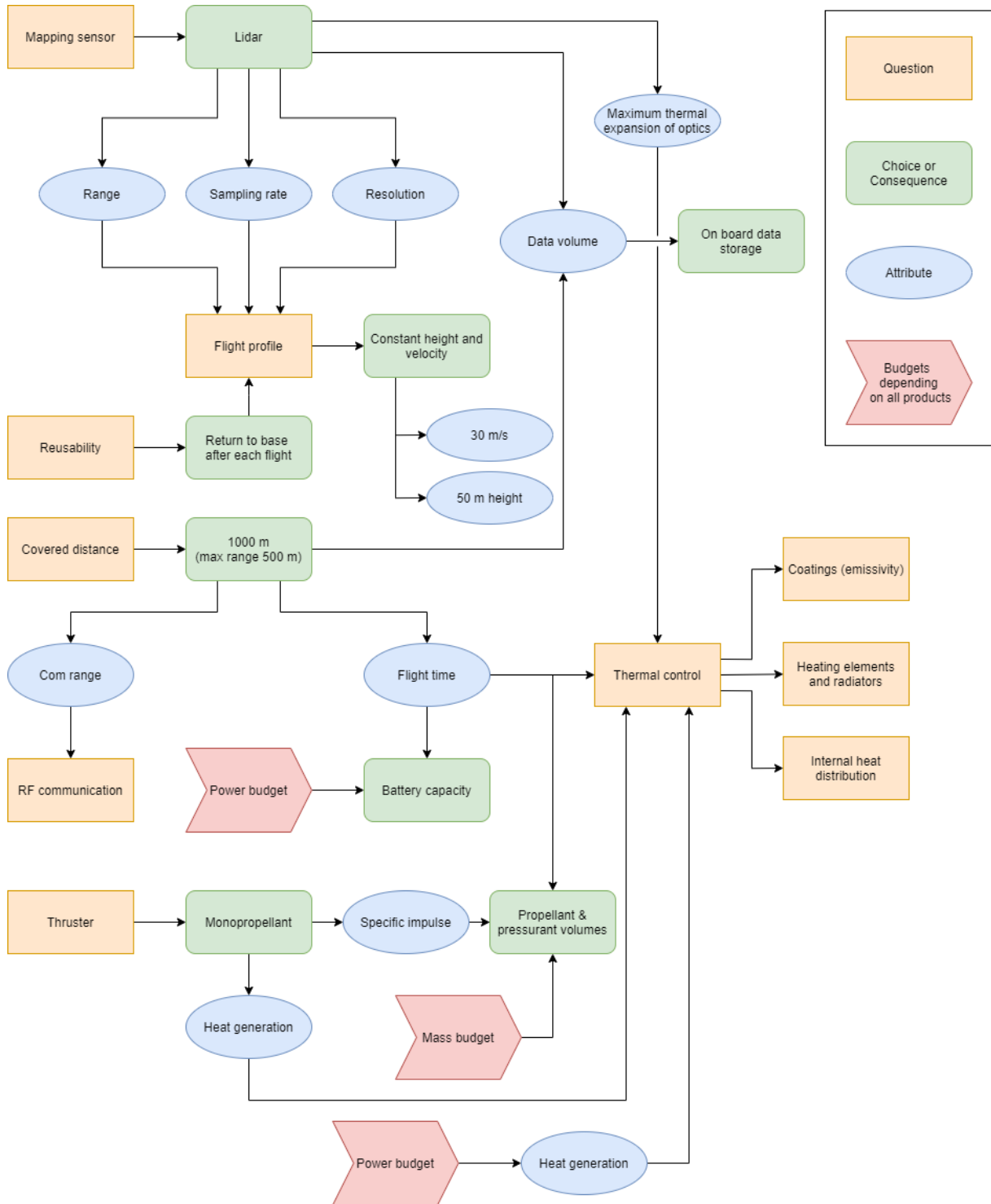


Figure 4: Initial analysis results and decision mind-map.

6 Drone design

To be able to analyze the system further and find the technological challenges, an initial design of the drone is made. This initial design helps for the visualization of how all the different parts influence each other and makes the writing of requirements and budgets easier. Several iterations of specifications and rapid designs are realized during the course of this project.

6.1 Decomposition in subsystems

The subsystem of the drone are defined as follows:

- AV - Avionics: Onboard computer (OBC), attitude control and object detection and avoidance
- CDH - Communication & data handling: Data processing, storage and transmission
- PL - Payload: 3D mapping and imaging instruments
- PR - Propulsion: thrusters, plumbing and tanks
- PWR - Power: Batteries and cables
- ST - Structures
- TH - Thermal

6.2 Functional decomposition and solutions

The first design step is to perform a functional decomposition and identify possible solutions for each function. In [Table 3](#), this is done by the means of a morphological matrix. The chosen solution for each function is highlighted in green. More details on the different components are given in [subsection 6.4](#).

Table 3: Morphological matrix of functions and solutions (selected one in green)

Function	Solutions					
C&DH	No on-board processing: storage only	On-board processing of flight data only	On-board processing of all data			
Mapping data communication	By radio during flight	By radio when landed	By cable when landed on drone base			
Attitude control	Reaction wheels	Multiple thrusters (RCS)	Spin stabilization	Momentum wheels	Control moment gyros	Thrust vectoring
Mapping	Visual (lighting)	Radar	Rotating Lidar	Flash Lidar	Thermal	Magnetic
Power source	Battery	Nuclear				
Charging	Solar	None	Drone base charging			
Propulsion technology	Mechanical	Mono propellant (hot)	Bi propellant	Solid Hybrid	Electric (ion)	Cold gas
Refueling and recharging (for reusability)	None	Pick up by rover	Landing on rover (drone base)			
Heating	Electrical	Selective exposure to the sun	Radioisotope heaters			
Ensure heat distribution uniformity	Fluid loops	Heat pipes	Heat capacities	Copper heat straps		
Control heat loss	Coatings	No contact with ground	Protective cover when not in use	All		
Thermal cycling	Materials with similar expansion coeff	Limit thermal cycle amplitude	Both			
Sensor pointing and stabilization	Dedicated gimbal and dampers	Using the drone's attitude control				

6.3 Product tree

The drone's design is kept as simple and compact as possible. An overview in form of a product tree is presented in [Figure 5](#).

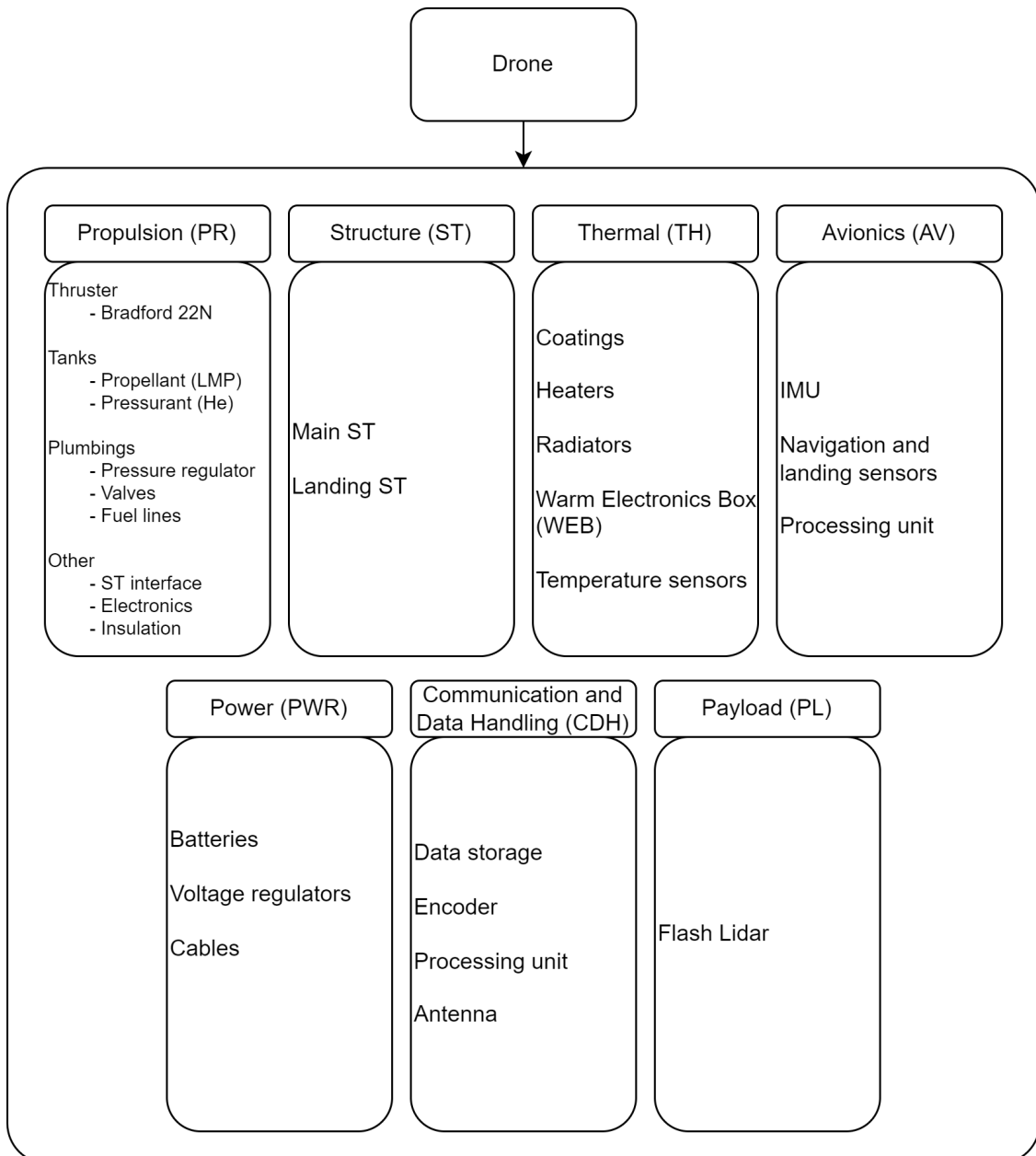


Figure 5: Product tree of the lunar drone.

6.4 Details for the different subsystems

The drone is decomposed into seven subsystems which are described below.

6.4.1 Propulsion

The propulsion system of the drone is of central interest in this study. As discussed in [subsection 5.1.2](#), a monopropellant system is selected for its combination of simplicity and efficiency. To control the attitude of the spacecraft, four small thrusters are used. The other options and their advantages, disadvantages are shown in [Figure 6](#). Other thruster arrangement options are discussed in [subsection B.1](#) of the Appendix.

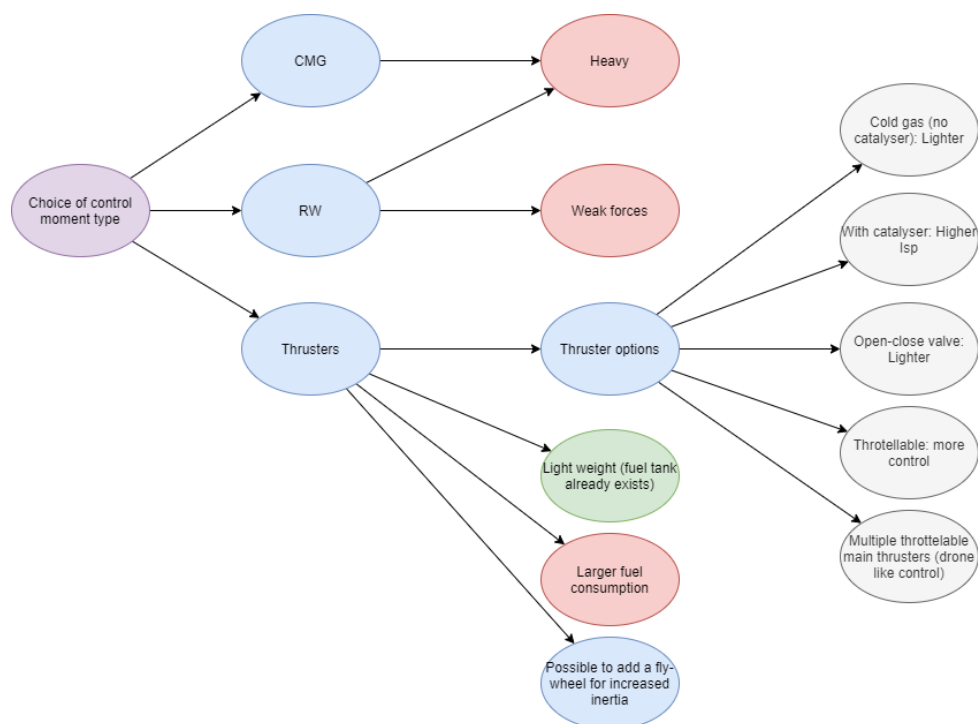


Figure 6: Choices and effects of spacecraft attitude control technologies.

In order to avoid dust generation directly underneath the drone where the mapping and flight sensors would be located, the thrusters are angled with respect to the z-axis of the drone and attached to its top. This is another advantage of using four thrusters to control the attitude of the drone. In addition, to allow for yaw-control of the drone, the thrusters should be offset with respect to the z-axis. A schematic representation of their arrangement is shown on [Figure 7](#). For simplicity reasons, the angles alpha and beta are set at 45 degrees for the propulsion simulations presented later in this report. However, the determination of optimized thruster angles requires more detailed investigation in the future.

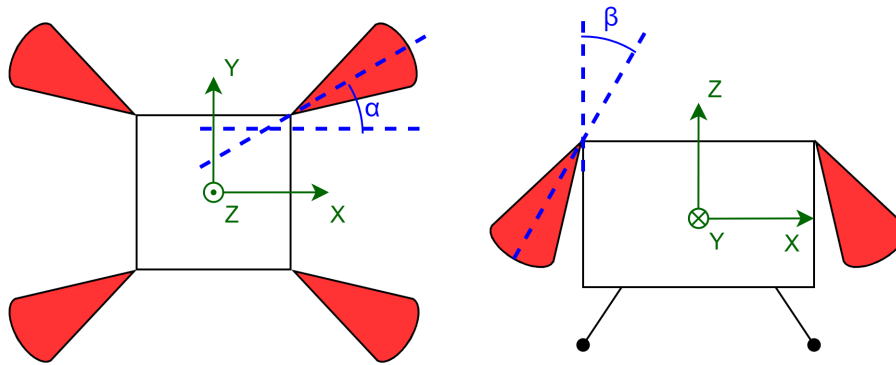


Figure 7: Top view (left) and side view (right) of the drone with its four thrusters (red). The x-axis is in the main direction of flight. Angles alpha and beta are at 45 degrees.

The main components of the chosen propulsion system of this first drone design are four 22N HPGP (High Performance Green Propulsion (HPGP)) Thrusters, manufactured by the Swedish company Bradford ECAPS [30]. These thrusters use the non-toxic LMP-103S propellant (a so-called "green propellant"). They have a thrust range of 5.5 to 22 Newtons and a specific impulse of 243-255 s in steady state. An overview of the main specifications can be found on Table 4. The combination of four thrusters provides a force of up to 88 N which is largely sufficient for the drone.

Table 4: Thruster main specifications [30]

Specification	Value
Propellant	LMP-103S
Propellant freezing point	-90 °C
Inlet pressure range	5.5 - 24 Bar
Thrust range	5.5 - 22 N
Nozzle expansion ratio	150:1
Steady state ISP (in vacuum)	243 - 255 s
Overall length	260 mm
Mass	1.1 kg
Pull-in voltage	28 ± 4 VDC
Regulated reactor ore-heating power	25 - 50 W (TBC)

Besides the thrusters, propellant and pressurant tanks are required, as a so-called regulated system is used as pressurization system: Since the thrusters are based on a pressure-fed cycle and because the pressure in the propellant tank would decrease over time with decrease of the propellant volume, a pressurization system is necessary to keep the engine input pressure constant. Two simple methods exist for this: a regulated system and a blowdown system. In the former, a separate pressurant gas is used in combination with a pressure regulator to push the propellant out of its tank and replace it. In the latter, the pressurant gas is stored in the same tank together with the propellant and physically separated by a diaphragm or a bladder [31, 32]. To have better control over the output pressure and thus over the resulting thrust, a regulated system is selected for the drone. Although

this system is heavier due to the higher amount of components needed, it is easier to control and to refuel, which is critical to make the drone reusable.

The exact masses and volumes of the pressurant and propellant tanks are calculated in the appendix subsection B.6 and are sufficient for two straight-line flights of 1000 m each, if the system is optimized. The pressurant insertion is controlled by a pressure regulator for better pressure control in the propellant tank. A simplified representation of the drone's propulsion system placement on the drone is depicted in Figure 8. A more detailed schematic diagram of the propulsion system on its own is represented in Figure 9. It is based on the Green Propellant Infusion Mission (GPIM) by NASA and other satellite propulsion systems [31, 33, 34].

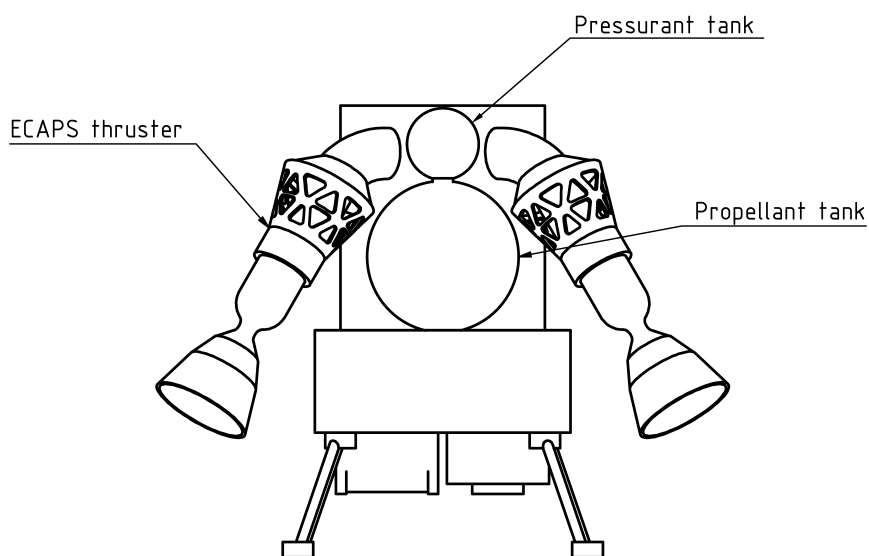


Figure 8: Illustration of the propulsion system of the drone. Note that components such as valves, tubes and pressure regulators are not represented.

6.4.2 Structure

The drone's structure needs to hold all the components in place with respect to each other. It also needs to have landing legs or other features that will interface with the drone base, including a hold down mechanism. Moreover, it should be made of materials with similar expansion coefficients to avoid any thermal stresses on the structure. No detailed structure has been developed in the scope of this project but several ideas were formulated.

One idea could be to use the titanium propellant tanks as part of the structure. The rest of the structure could therefore also be made of titanium.

From a thermal perspective, it would also make sense to isolate the different subsystems such as the thrusters, the rest of the propulsion system and all the electronics/sensors. For example, the heat of the thrusters firing should not be conducted into the rest of the drone. The electronics and sensors could also be placed in a Warm Electronics Box (WEB) to better control their temperature.

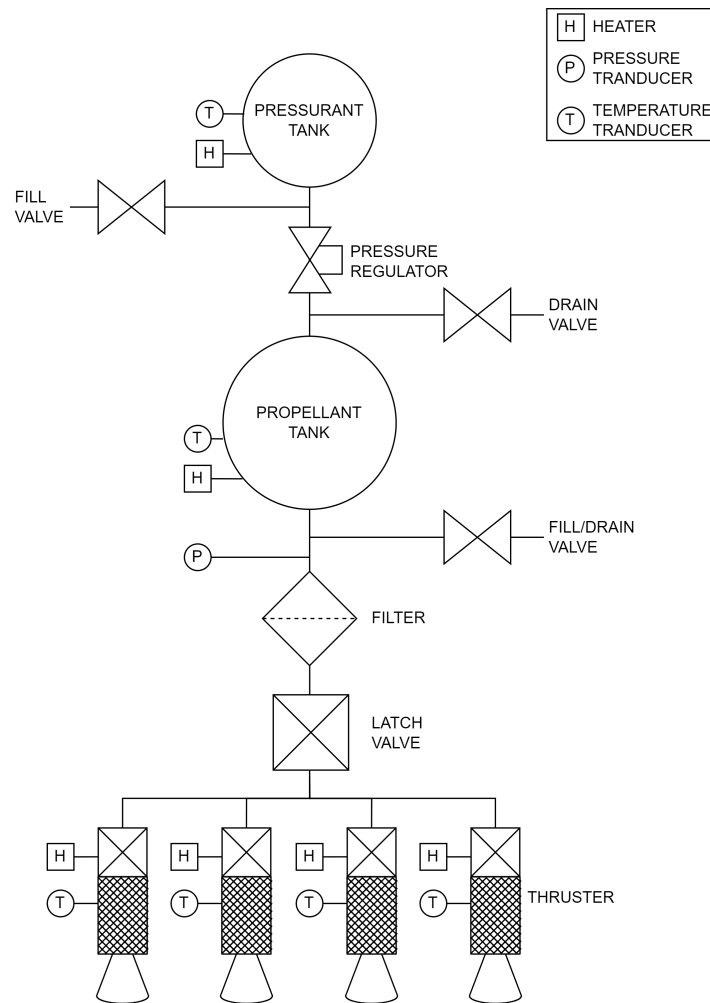


Figure 9: Schematic diagram of the drone's propulsion system (based on [33] and [34]).

It would also be interesting to allow for a standardized payload attachment, such that the Lidar could be changed for other instruments. This would make the drone very flexible and future proof. ESA for example is currently working on standardized electrical, thermal and mechanical interfaces for their EL3 mission [24].

6.4.3 Thermal

As seen in section [subsection 5.1.3](#), the drone needs to be thermally monitored and controlled to stay within its operable temperature range. The latter is defined by the components used in the drone. A general overview of temperature ranges for different components is given by Larson et al [31]. The relevant ones for the drone are listed in [Table 5](#) below. This means that a combination of active and/or passive thermal control systems is necessary to stay within the desired temperature range of about 0 to 50 °C.

Table 5: Typical operational and survival temperature ranges of various components according to Larson et al [31], adapted and extended by the authors

Component	Operational	Survival
Batteries [35]	-30 to 60 °C	-40 to 60 °C
Power Box Baseplates	-10 to 50 °C	-20 to 60 °C
C&DH Box Baseplates	-20 to 60 °C	-40 to 75 °C
Antennas	-100 to 100 °C	-120 to 120 °C
Solar Panels	-150 to 110 °C	-120 to 120 °C
Tanks [36]	0 to 50 °C	-
Propellant (LMP-103S)	-5 to 60 °C	-90 to 120 °C

The main challenge for the thermal system of the drone is the tuning of the passive components (heat capacity, emissivity and absorptivity) to reduce the needed power of the active thermal system (heaters). Since cooling the spacecraft would require heavy radiators, it is preferable to use heaters when necessary. Therefore, the drone should be able to evacuate all the heat when flying in the sunlight. The critical components should be placed close together in a Warm Electronics Box (WEB) and a "propulsion box" to keep them at an operable temperature by using active electrical heaters. This is especially necessary when flying into PSRs. In addition, heat straps, often used in small satellites [23], can be used to help distribute the heat via conduction (example shown on Figure 10). Finally, the absorptivity and emissivity of the drone can be controlled with help of special paint and surface coatings which are commonly used in the aerospace industry. Calculations of evacuated thermal power with respect to the emissivity and absorptivity as well as temperature variations of the drone during a flight are presented in Appendix C. These calculations are based on a significant number of assumptions, such as the uniformity of temperature distribution in the drone. Therefore, a more detailed analysis is still required to define exactly which components should be used where and how.

The four thrusters are one of the main heat sources in the system (together with sunlight and electrical power consumption). The removal of heat produced by these thrusters represents another challenge for the thermal system but after a discussion with Prof. Hiroyuki Koizumi from University of Tokyo, a specialist in space propulsion, it appears to be feasible to dissipate heat of the thrusters via radiation. The engine bell and combustion chamber are allowed to become red hot and radiate their thermal energy into space while thermal conduction to the spacecraft structure can be kept very small.

Finally, when the drone is not in use, it should be protected under an insulating cover. This is due to the large temperature losses of the drone when it is not used and no heat is generated internally. Figure C.4 shows this decrease of temperature if the drone is in the shadow and not protected. More details on the insulating cover are given in section 7.

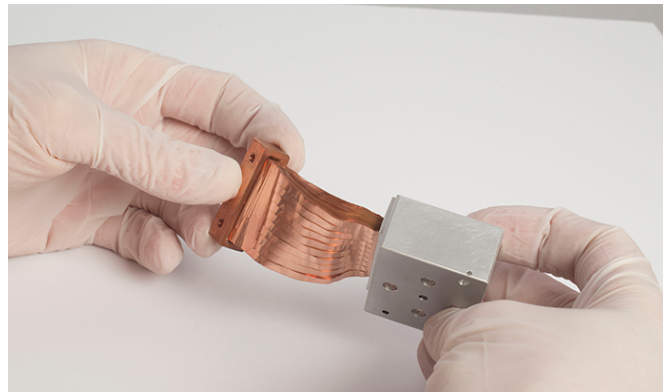


Figure 10: Flight proven copper thermal straps by the Space Dynamics Laboratory (SDL) [37].

6.4.4 Avionics

No detailed studies or calculations of the avionics have been performed in the scope of this project. It is regarded as a black box with a mass of 0.5 kg (with an additional contingency of 20%) and a power consumption of 10 W (30% contingency). However, it is considered that technologies used for space avionics are sufficiently developed and flight-proven to not pose any problems or limitations in the development and conception of this subsystem in the future. Algorithms used to control the thrusters for example can be based on the ones used in modern drones with four propellers, as well as hazard detection and avoidance algorithms.

The avionics subsystem needs to guarantee safe take-off, exploration flight and landing of the drone. For this purpose, it should be equipped with Inertial Measurement Unit (IMU)s and a range finder, and also process the 3D mapping data for navigation and object detection and avoidance. For the take-off and landing, an optical imager will be used on the underside of the drone to track corresponding lights installed on the drone base. The latter will serve as optical markers to determine relative position (distance and height) of the drone with respect to the base. This method has been extensively studied with the development of unmanned aerial vehicles (UAVs) [38].

6.4.5 Power

The drone's power system is set at a standard bus voltage of 28 V, which is commonly used in the aerospace industry. The power is provided to the drone's subsystems by space-adapted rechargeable lithium-ion batteries. These are then recharged by the rover's power system via the drone base to ensure reusability of the drone (see [section 7](#)). Detailed calculations for the batteries and power consumptions are given in [Appendix D](#). The *Saft MP 144350 xlr Rechargeable Li-ion* batteries have been selected for the drone application. Eight of these 3.65 V batteries are necessary to obtain the desired voltage. They allow for about 13 minutes of operation time and have a total mass of 0.8 kg. Note that these numbers are based on approximate power consumption values given in the datasheets and that "worst-case" values are used for the calculations (e.g. peak power consumption of the thrusters of 50 W each).

6.4.6 Communication and data handling

Communication between drone and base can be separated into two modes: Communication when the drone is docked on the base and in-flight communication. During flight, the drone captures 3D mapping data of the lunar ground with its Lidar system (see [subsection 5.1.1](#) and [subsection 6.4.7](#)). This data is not only temporarily stored on the drone, but also directly processed by its On-Board Computer (OBC) to determine flight parameters such as position and altitude and to be used by the hazard detection and avoidance system. The data sent to the base during flight is limited to drone health, position tracking, power and propellant consumption (housekeeping data). The data received by the drone are health checks and commands (e.g. abort mission and return to base). When docked to the base and connected via cable, the drone transmits the mapping data to the rover. Housekeeping data is continuously sent and monitored as well.

6.4.7 Payload

The main payload is a flash Lidar used as a mapping sensor, as described in [subsection 5.1.1](#). The high resolution map can then be used by the rover to choose its exploration path, especially into PSRs. As mentioned previously, lightweight flash Lidars for space applications are in development and should become available in the near future. These new Lidars are expected to weigh below 4 kg. Detailed calculations giving requirements on the Lidar's resolution and imaging frequency are given in [Appendix A](#).

Additionally, the Lidar should be interchangeable with other payloads and sensors. This will make the drone more flexible. It will be able to adapt to new needs and do different types of missions. A potential outlook and more ideas are given in [section 10](#).

6.5 N2 chart

All of the design choices somehow influence the other decisions. To visualize how these decisions affect each other, an N2 chart was created. The mission defining choices are highlighted in green on the diagonal of the chart. The influences are marked with an "x" when trivial and more details are given for the other pairs.

		Propulsion					Electronics				Thermal (flight)			Flight profile				Structure		Drone support equipment					
		Thruster type	Propellant	Propellant volume	Engine weight	Tank and valves weight	Mapping sensor	RF communication	Data storage	Battery	Operating temperature	Emissivity	In Flight Temp. Change	Control	Distance	Height	Speed	Total weight	Material	Flame diverter	Fueling	Charging	Data transmission	Storage temperature	Total weight
Propulsion	Thruster type	Mission defining	x		x	# components			Power consumption			Heat generation	Throttleyability					Loads and temperature	Exhaust gas temperature						
	Propellant			isp						Melting point										# of connection			Freezing	isp	
	Propellant volume					size														Propellant volume				Number of flights	
	Engine weight																x								
	Tank and valves weight																x								
Electronics	Mapping sensor					Mission defining	Data volume	Power consumption	x		Expansion of optics			Sensing range	Sampling rate	x					Data volume	x			
	RF communication							Power consumption									Interference				x	x			
	Data storage																					x			
	Battery								x							x				Time		x	Capacity		
Thermal (flight)	Operating temperature										x													Thermal dependance	
	Emissivity																	Coatings					x		
	In Flight Temp. Change											Heat transfer						Thermal fatigue							
Flight profile	Control																								
	Distance			Flight time			x	Data volume	Autonomy			Flight time	Mission defining									Data volume			
	Height																								
Structure	Speed			Flight time																					
	Total weight			x								Heat capacity													
Drone support equipment	Material															x									
	Flame diverter																							x	
	Fueling					x																		x	
	Charging																								
	Data transmission																								
	Storage temperature																							x	
Total weight																									

Figure 11: N2 chart.

7 Drone base design

The design of the drone base is out of the scope of this project. However, certain components, interfaces and functions have been identified during the design of the drone itself.

7.1 Product tree

The drone base's first design is represented by the product tree shown in [Figure 12](#).

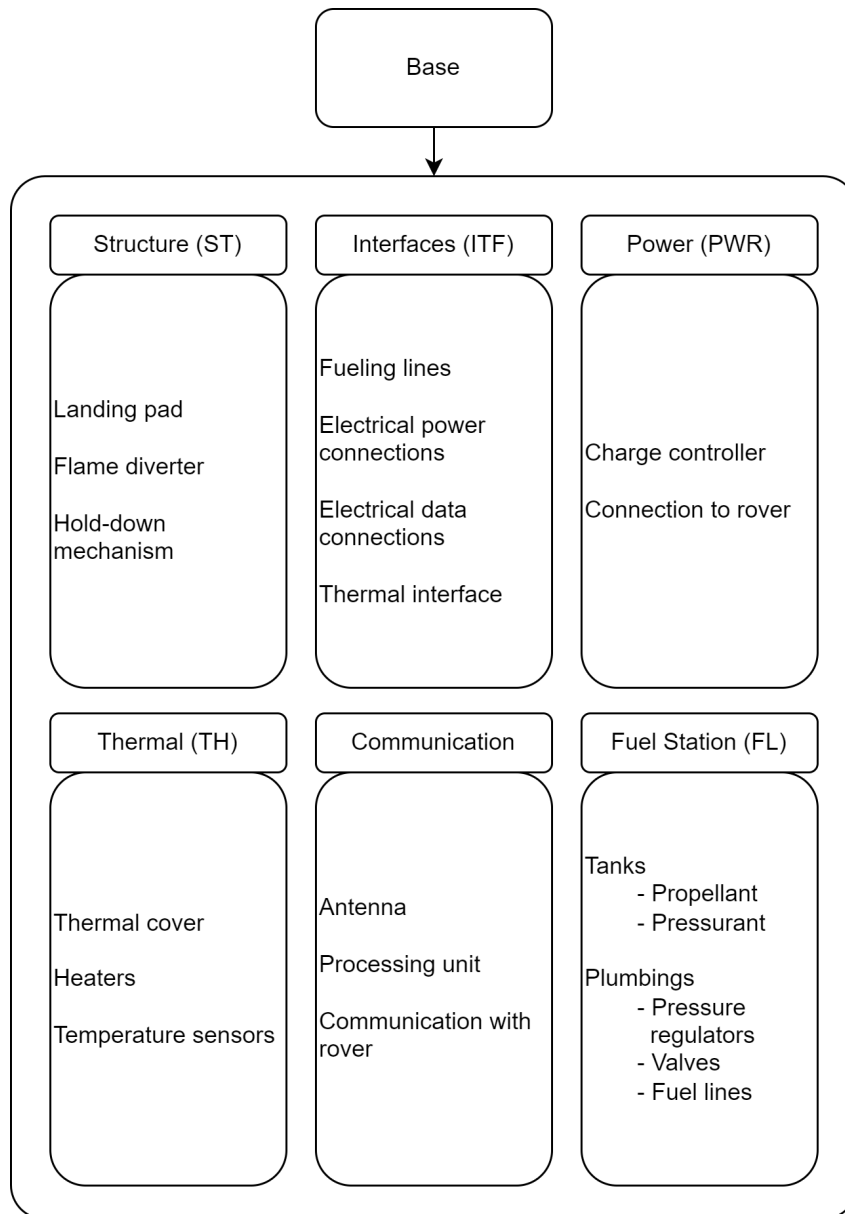


Figure 12: Product tree of the drone base module.

7.2 Decomposition in subsystems

The subsystem of the drone base are defined as follows:

- CDH - Communication & data handling: Data transmission to the rover
- IF - Interfaces with rover: Mechanical, power and signal interface between base module and rover
- PR - Propulsion: Propellant and pressurant storage
- PWR - Power
- ST - Structures
- TH - Thermal: Thermal and radiation protection for the drone

7.3 Drone base functions

The drone base has four main functions:

- Provide a shelter for the drone when not in use, i.e.:
 - Attach/secure the drone during flight to the Moon and rest of the rover mission with a reversible hold down and release system.
 - Insulate the drone to prevent large temperature losses with a radiation cover.
 - If possible, connect to drone to the thermal system of the rover.
- Provide a take-off and landing base, including:
 - A flame diverter to direct the thrusters exhaust away from the rover.
 - Features to ease the landing of the drone (for example optical markers or lights)
- Provide a data connection to transfer the mapping sensor data from the drone to the rover.
- Allow for the refuelling and recharging of the drone to make multiple flight possible and therefore have:
 - Propellant and pressurant tanks.
 - Fuel line connection and disconnection systems.

The main challenge for this drone base will be to make it as compact and as independent as possible, such that it can easily be integrated on various rovers and be used for other future applications. The size of the refuelling tanks could be adapted to the number of flights the drone is expected to perform (e.g. ten flights). Solar cells on the cover for additional power generation could also be imagined.

8 System Engineering Results

Based on the decisions taken and the design choices made in the previous chapters, a more in-depth and detailed design and concept of the system can be derived. Specifically, a detailed Concept of Operations (ConOps) is presented, as well as preliminary mass and power budgets and high level requirements. These results can be used as a starting point of future, more detailed development projects around the drone and its base.

8.1 ConOps

The ConOps of the lunar reconnaissance drone is presented on [Figure 13](#). It can be subordinated to the rover's ConOps and is composed of seven main phases of operations:

0. Launch and landing on the Moon: Pre-mission phase of the drone, from launch on Earth to Lunar Orbit Insertion and deployment of the rover on the lunar surface. The drone module is deactivated. Drone is covered and protected by the drone base. The drone is secured to the landing pad by the hold-down system.
1. Stand-by mode: The drone is activated and in a low-power mode. Only essential data of the drone is monitored. The drone is covered and protected by the drone base. The drone is secured to the landing pad by the hold-down and release system.
2. Flight preparation and deployment: The drone is being prepared for flight, propulsion system is fueled and power system is charged, the flight instructions are uploaded to its avionics subsystem. The cover is opened and the fully charged and fueled drone disconnects from the base.
3. Take-off and vertical ascent: The drone propulsion system fires, vertical lift-off is followed by ascent until the desired height of 50 m is reached. The on-board Lidar start scanning the ground at a minimum frequency of 300 Hz and the horizontal flight trajectory is initiated.
4. Horizontal flight: The Lidar scans and maps the lunar surface in 3D. Drone transmits data to the base (drone's propellant and power state, position, altitude and velocity). The horizontal velocity reaches 30 m/s at maximum and a total horizontal distance of about 1 km (outward and return) is covered.
5. Vertical descent and landing: Drone returns to the base. Using an on-board 2D camera, it visually tracks according tracking lights on the base, descends and lands on the base module. The drone is then secured to the pad by the hold-down mechanism and the cover of the base is closed. Fueling, power and signal lines are connected to the drone. Mapping data is transmitted to the rover, while the drone is refueled and recharged.
6. End-of-life phase: Propellant and pressurant reserves of the base allow for ten flights of the drone. Afterwards, the drone module can be stored for later use once new propellant is available.

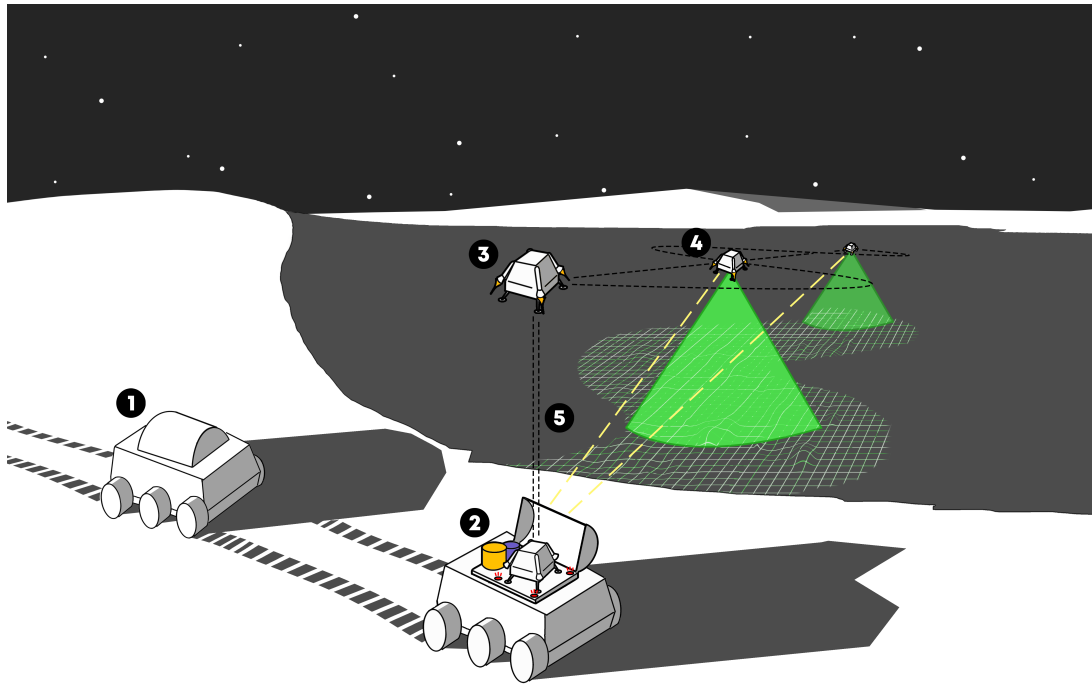


Figure 13: Lunar reconnaissance drone module: Concept of Operations. 1. Stand-by mode; 2. Flight preparation and deployment; 3. Vertical ascent; 4. Horizontal flight and surface mapping; 5. Vertical descent and landing.

8.2 Budgets

Preliminary budgets for mass and power are presented in [Table 6](#) and [Table 7](#) respectively. Note that contingencies of 20% or 30% are added to all subsystems which have not been designed in detail, while the propulsion subsystem already includes contingencies in the detailed calculations not shown here.

8.2.1 Preliminary Mass Budget

The mass budget for the propulsion subsystem is calculated following the procedure proposed by Larson et al [31]. The propellant mass used is sufficient for two straight-line flights of 1000 m, if the system is optimized. The detailed calculations can be found in [Appendix B](#). On top of individual contingencies of 20% on each subsystem, a 10% global margin is allocated for the entire system.

8.2.2 Preliminary Power Budget

The power budget is estimated based on datasheets provided by manufacturers for specific components, on similar project reports or on personal experience of the authors. For uncertainty reasons, a contingency of 30% is added to all subsystems as well as a 20% global margin.

Table 6: Preliminary mass budget

Subsystem	Component	Value	Unit	Contingency
Propulsion	Thrusters	4.40	kg	
	Propellant	2.0	kg	
	Propellant tank	0.074	kg	
	Pressurant	0.021	kg	
	Pressurant tank	0.045	kg	
	Piping, valves	1	kg	
	Subtotal	7.54	kg	20%
Payload	Lidar	2	kg	20%
Thermal		1	kg	20%
Structure		1	kg	20%
Avionics		0.5	kg	20%
C&DH		0.25	kg	20%
Power	Batteries	0.8	kg	
	Cables, etc.	0.25	kg	
	Subtotal	1.05	kg	20%
Sum		16.01	kg	
Global margin		10%		
Total		17.61	kg	

Table 7: Preliminary power budget

Subsystem	Component	Value	Unit	Contingency
Propulsion	Thrusters	200	W	30%
	Valves	5	W	30%
	Regulators	5	W	30%
Payload	Lidar	30	W	30%
Thermal	Heaters	5	W	30%
Avionics		10	W	30%
C&DH		20	W	30%
Sum		357.5	W	
Global margin		20%		
Total (cont. incl.)		429	W	

8.3 Requirements

In order to facilitate the drone and base design process, a set of high level requirements are defined. They act as a first reference at the beginning of the project and are revisited and adapted accordingly when required throughout the process. The requirements are presented in [Table 9](#) and [Table 10](#) below and are separated in Drone Requirements and Drone Base Requirements. Note that both are of preliminary nature and require deeper reflection in the future. The abbreviations under the "system" column are the acronyms of the different subsystems. SYS stands for a general requirement on the entire system.

8.4 Risk analysis

Although not all subsystems are designed in detail at this stage of the project and more time needs to be allocated for this in the future, a preliminary risk analysis can be realized here. For this, a simplified Failure Mode and Effects Analysis (FMEA) is done based on the theory learned in the ENG-421 EPFL course (*Fundamentals in Systems Engineering*) and in the CS-487 EPFL course (*Industrial automation*), a method also used by the EPFL Rocket Team (ERT), in which both of this report's authors are active.

In the bottom-up FMEA approach, each component is analyzed and potential failures listed. To each failure point, a probability value (from 1 [improbable] to 5 [near certainty]) and a severity value (from 1 [negligeable] to 5 [catastrophic]) is attributed, from which a risk level can be deduced (from 1 to 12). The correlations used between probability and severity are given in [Table 8](#). The color code indicates whether the addressed point presents a high risk (redish colors) or not (greenish) for the mission. For each failure, a mitigation method is added.

Table 8: Severity matrix and risk color code

		Risk Level				
		1	2	3	4	5
Probability	5	2	3	6	9	12
	4	2	3	5	8	11
	3	1	2	4	7	10
	2	1	2	3	5	8
	1	1	1	2	3	5
		1	2	3	4	5
		Severity				

A detailed list of each system component can be found in [Appendix E](#). The major points resulting from this analysis are:

- The highest risk is identified for the failure of the Lidar system with a value of 8, as it represents the main objective of the reconnaissance drone. Scanning of the lunar ground can fail due

to various reasons, but mainly either due to dust limiting the laser operation or due to failure of the Lidar system itself. To mitigate the first reason, dust dispersion needs to be reduced or prevented. For this, the thrusters are angled away from the drone and a fire deflector used on the drone base. For the second reason, the Lidar system needs to be extensively tested before the mission in order to guarantee its nominal operation on the Moon.

- Another risk due to dust dispersion relates to the optical tracking system of the drone, which is used for take-off and landing. Here, if tracking of the according lights installed on the base fails, especially landing becomes very difficult. Again, dust dispersion needs to be mitigated.
- A further high risk is found in the propulsion system: As the flight of the drone relies on all four thrusters, one or more defect thrusters can have a significant impact on the mission. If one thruster does not operate correctly, an "emergency flight mode" could be implemented, which allows for the drone to return to the base with only three active thrusters, but very limited control possibilities. If more than one thruster fails, the mission cannot be executed and fails. To prevent thruster problems, extensive testing is required and fire tests necessary before each flight.
- Another risk concern the power capacity of the batteries, which can be mitigated with redundant batteries.
- All moving mechanisms in space represent a high risk due to cold-welding and lubrication aspects. These mechanisms include the drone-base interfaces (power, propulsion and data), the radiation cover and the hold-down mechanism of the base module. Again, extensive testing and the use of appropriate lubricants is necessary, as some failures (e.g. cover does not open) mean permanent mission failure.

Table 9: Preliminary drone requirements

ID code	System	Short	Detailed description	Verification
2021-D-AV-01	AV	Autonomous landing	The drone shall be capable of autonomous landing on the drone base	Testing
2021-D-AV-04	AV	PL independence	The drone shall be independent of its payload	Demonstration
2021-D-AV-02	AV	Position tracking	The drone shall track its position in space during flight	Testing
2021-D-AV-03	AV	Return to base	The drone shall be capable to abort its flight mission and return to the base autonomously	Testing
2021-D-AV-05	AV	Obstacle detection	The drone should use the acquired 3D mapping data for obstacle detection and avoidance during flight	Testing
2021-D-AV-05	AV	Altitude acquisition	The drone shall measure its altitude independently of the mapping sensor for object avoidance during flight	Testing
2021-D-CDH-01	CDH	In-flight communication	The drone shall use wireless radio antennas to transmit data directly to the rover when within sight	Demonstration
2021-D-CDH-02	CDH	Rover communication	The drone should always be in sight with the rover	Analysis
2021-D-CDH-03	CDH	Com range	The communication range of the drone shall be at least 2 times the flight range	Testing
2021-D-CDH-04	CDH	Hovering strategy	The flight shall ensure direct communication with the rover and household and flight data transmitted to the rover	Demonstration
2021-D-CDH-05	CDH	Data storage inflight	3D mapping data shall be stored on the drone during the flight	Demonstration
2021-D-CDH-06	CDH	Data transmission	3D mapping data shall be transmitted to the rover after landing on the base	Demonstration
2021-D-PL-01	PL	Payload mapping resolution	The payload shall provide a mapping resolution of <0.5 m/pixel	Demonstration
2022-D-PL-02	PL	Mapping range	The drone's flight altitude shall be within the mapping range	Testing
2021-D-PL-03	PL	Mapping technology	The mapping should be three-dimensional	Demonstration
2021-D-PL-04	PL	Continuous mapping	The payload shall provide a continuous mapping under the flight path	Demonstration
2021-D-PL-05	PL	Adaptability	The drone's payload should be interchangeable with instrumentation of similar size and power requirements	Testing
2021-D-PR-07	PR	Drone horizontal velocity	The maximum horizontal flight velocity shall lie below 50 m/s	Testing
2021-D-PR-08	PR	Flight altitude	The drone shall flight at 50 m (± 10 m) during the mapping	Testing
2021-D-PR-01	PR	Dust dispersion	The propulsion system shall not limit the mapping due to dust dispersion	Testing
2021-D-PR-02	PR	Flight range	The propulsion system shall be capable of covering a horizontal distance of at least 1000 m	Testing
2021-D-PR-03	PR	Propellant toxicity	The propulsion system should avoid the use of highly toxic propellants	Inspection
2021-D-PR-04	PR	Refuability	The propulsion system shall be refuability by the drone base	Testing
2021-D-PR-05	PR	Propellant freezing pt.	The propellant's freezing point shall be below -50°C	Testing
2021-D-PR-06	PR	Pressurant freezing pt.	The pressurant's freezing point shall be below -50°C	Testing
2021-D-PWR-01	PWR	Power capacity	The power system shall provide all energy required for one flight (with contingency)	Testing
2021-D-PWR-02	PWR	Rechargeability	The power system shall be rechargeable by the drone base	Testing
2021-D-ST-01	ST	Storage size	The drone's volume shall fit within the drone base	Inspection
2021-D-SYS-01	SYS	Dust proofness	The drone shall be completely dust proof against lunar regolith (equivalent rating: IP6)	Testing
2021-D-SYS-02	SYS	Landing slopes	The drone shall be able to land on its base with inclinations up to 25°	Testing
2021-D-SYS-03	SYS	Mass & volume	The drone shall not exceed a mass of 20 kg	Demonstration
2021-D-SYS-04	SYS	Rover integration	The drone should deploy without help of an active onboard deployment mechanism on the rover	Demonstration
2021-D-TH-01	TH	Stand-by temp.	The drone's thermal system shall keep the drone's temperature between [-20°C, 60°C] during stand-by phase with help of a radiation cover on the drone base	Testing
2021-D-TH-03	TH	Thermal control	The drone shall be equipped with active thermal control	Demonstration
2021-D-TH-04	TH	Operational temp.	The drone's and thermal system shall keep the drone's temperature between [0°C, 50°C] during operation phase	Testing

Table 10: Preliminary drone base requirements

ID code	System	Short	Detailed description	Verification
2021-B-CDH-01	CDH	Data reception & transmission	The base shall receive the drone's data and transmit it to the rover by cable	Testing
2021-B-CDH-02	CDH	Com	The base shall send commands and receive flight and household data from the drone during the flight	Testing
2021-B-IF-01	IF	Power interface	The base shall allow for the drone to be charged by the rover's power subsystem	Testing
2021-B-IF-02	IF	Connection system	The base shall be equipped with a mechanically actuated connector system for the drone for power, propulsion and data	Testing
2021-B-IF-03	IF	Standard interfaces	The base should be adapted to standard power, thermal and data interfaces to be defined by space agencies in the future	Demonstration
2021-B-PR-01	PR	Propellant capacity	The base shall hold propellant tanks to refuel the drone's propellant tank at least 10 times	Demonstration
2021-B-PR-02	PR	Pressurant capacity	The base shall hold pressurant tanks to refuel the drone's pressurant tank at least 10 times	Demonstration
2021-B-ST-02	ST	Deflector	The base shall protect the rover from the drone's propulsion system	Testing
2021-B-ST-03	ST	Hold-down mechanism	The base shall hold down the drone while in standby mode	Testing
2021-B-TH-01	TH	Thermal protection	The base shall protect the drone from radiation and low temperatures	Testing

9 Future work, open questions and limitations

The main limitations and open questions to be addressed in the future are of different nature and concern various aspects of the drone project.

One first study required would be a detailed analysis of the propulsion system with in-depth simulations and thruster arrangement trade-off. The limitations and possible improvements of the flight simulations are already discussed in [subsection B.8](#). As for the thruster arrangement, an optimal balance between high precision control and propellant efficiency needs to be determined. Another point to be studied in the future are possible off-nominal flight performance situations, such as failure of one or several thrusters, and how they can be mitigated or prevented. Possible solutions would be to implement an emergency or reduced-thrust flight mode where the drone can return to the base using only three thrusters instead of four, or to increase the amount of thrusters used. Here, a detailed trade-off with calculatory justifications is required.

Concerning the thermal subsystem of the drone, the analysis done in this report is limited and simplified to some extent (see [Appendix C](#)). A detailed thermal study of the drone with given structure and materials, localized heat sources and sinks would be necessary in order to further develop the drone. The effect of sunlight would also have to be included in the analysis, and one interesting aspect to be explored would be the use of radiators for heat dissipation in this context.

Finally, the main aspect to be developed remains the base of the drone. Since it acts as interface between drone and rover, it has to be adapted to rover designs and standards. A flame deflector to protect the rover needs to be conceived as part of a thermal study of the drone base. A reliable connection mechanism to recharge and refuel the drone as well as a hold-down system have to be developed. Fuel tank masses and volumes need to be calculated and the weight of the base optimized. The radiation cover design has to be investigated and its opening and closing mechanism thought of. A communication subsystem with the drone with temporary data storage is also required in the base's design. From all this, detailed drone base system requirements have to be derived. They will determine if such a drone plus base system is feasible for lunar exploration or if the ConOps has to be adapted.

10 Author's opinion and outlook

By doing this project, the authors learned about the main challenges of lunar exploration, specifically at the lunar poles, and how to apply the basics of system engineering to a preliminary study of a lunar reconnaissance drone. The general result of the study suggests that it is feasible to use small drones such as Ingenuity on the Moon, though with a different propulsion technology which renders the reusability more challenging. With the idea of a complete drone module package consisting of a drone and a base, it is possible to offer a flexible solution to lunar exploration not only for rover missions, but also for future lunar bases and facilities. The idea of modularity of the drone's payload allows for other instruments to be used and therefor other missions types to be addressed. For example,

surveillance of Moon base construction by robots or aid in future rescue missions can be imagined if the system is developed further. The drone could also be used to explore lunar caves and lava tubes with more advanced mapping and trajectory planning algorithms. To extend the range and efficiency of the drone system, several drones could be deployed at the same time. In the far future, the drone system could also be applied to other moons and planets and help explore our solar system.

11 Conclusions and discussion

In this semester project report, a preliminary concept study of a lunar reconnaissance drone was realized using Systems Engineering tools and approaches. These included the use of morphological matrices and trade-off tables that helped the author's proceed in a structured and efficient manner. Several decision and consequence mind maps have been drawn to keep track of the choice's justification. The work was mainly focused on the design of a drone with a mapping payload in the form of a Lidar to explore Permanently Shadowed Regions (PSR) and regions with high terrain inclinations. These regions can indeed not be mapped from orbit with a sufficient resolution to plan exploration rover trajectories. Therefore, a lunar reconnaissance drone would definitely be useful to assist rovers on the Moon meant to go into PSRs.

The preliminary study of the lunar reconnaissance drone shows that its realization is in principle feasible. The main aspects defining the mission (i.e. propulsion, thermal and mapping) have been addressed and analyzed with reasonable assumptions. At this stage, the results obtained suggest that the mission is feasible with currently or soon-to-be available technology. Secondary aspects such as structure or avionics are kept as "black boxes" in the project and are points to be developed in the future.

One potential ConOps is analyzed in this report. In the situation that the rover is on the edge of a PSR and a trajectory into PSR needs to be determined, the drone can be deployed and take off from its base which is attached to the rover. It then flies into the PSR at an altitude of approximately 50 m AGL while mapping the area below itself. The flight is performed at a constant height to stay within the range of the Lidar and to ease the data analysis. The horizontal velocity is defined by the sampling rate of the mapping sensor and has been estimated to be at maximum 30 m/s. The horizontal distance that can be covered is estimated to be about 1000 m, which is sufficient to map a region of 250 m into the PSR (this is the distance into a PSR the EL3 rover is designed for).

Several conclusions were made from the initial feasibility research on the propulsion and thermal systems. For the flight described above, the required propellant mass (1 kg) is low compared to the rest of the drone's weight (around 15 – 20 kg). It is therefore critical to reduce the mass of the remaining systems on the drone such as:

- The power system by using small batteries that are recharged after each flight and by avoiding the need of solar panels.
- The communication system by storing the data on board and using only a small in flight communication antenna.

- The thermal system by using heaters when the drone is in the shadow instead of radiators for when the drone is in the sun, and by shielding it when not in use.
- The propellant tanks by keeping their volume small, just enough for one flight, and refuelling the drone once it has landed on its base.

Moreover, the drone should be kept between 0 and 50 °C to ensure its components operate well. By performing the thermal analysis, it became clear that getting rid of extra heat would become the main challenge. Since the drone is only cooled by radiation and its surface is limited, the main challenge is to remove extra heat during a flight in the sunlight. Surface coatings with high radiative emissivity and low absorptivity should be used. On the other hand, when the drone flies into a PSR, it will loose too much heat due to radiation and electric heaters shall be installed in strategic locations. Critical systems could also be isolated in insulated boxes to reduce heating power. When not in use and not heated, the drone's temperature will drop rapidly, up to 80 °C in two hours. Therefore, it should be insulated by a heat shield/cover.

All these aspects motivate the design of a drone plus base system. The drone base would act as a landing pad and flame deflector to reduce the dust being propelled by the engine exhaust. Moreover, it would ensure the reusability of the drone for multiple flights by implementing refuelling, recharging and data transfer interfaces. This drone base has not been studied in detail in the scope of the project and therefore still requires a lot of work, especially to determine its feasibility and budgets. The results of this future study will show if such a system can be implemented on a rover or if the drone's mission ConOps has to be modified.



Figure 14: Illustration of the drone (Original image: X Energy).

References

- [1] National Aeronautics and Space Administration (NASA). *Who has Walked on the Moon?* NASA Solar System Exploration. Apr. 28, 2021. URL: <https://solarsystem.nasa.gov/news/890/who-has-walked-on-the-moon> (visited on 01/04/2022).
- [2] NASA: *Artemis*. NASA. URL: <https://www.nasa.gov/specials/artemis/index.html> (visited on 01/04/2022).
- [3] V. T. Bickel et al. "Peering into lunar permanently shadowed regions with deep learning". In: *Nature Communications* 12.1 (Sept. 23, 2021), p. 5607. ISSN: 2041-1723. DOI: [10.1038/s41467-021-25882-z](https://doi.org/10.1038/s41467-021-25882-z). URL: <https://www.nature.com/articles/s41467-021-25882-z> (visited on 09/25/2021).
- [4] Janos Biswas, Simeon Barber, and Thibaud Chupin. *Exploring the Moon with the Lunar Volatiles Mobile Instrumentation – Extended (LUVMI-X) Platform*. Jan. 31, 2020.
- [5] Abigail Tabor. *Ice Confirmed at the Moon's Poles*. NASA. Aug. 17, 2018. URL: <http://www.nasa.gov/feature/ames/ice-confirmed-at-the-moon-s-poles> (visited on 01/04/2022).
- [6] National Aeronautics and Space Administration (NASA). *Mars Helicopter*. 2022. URL: <https://mars.nasa.gov/technology/helicopter/> (visited on 01/04/2022).
- [7] Sarah L. (Sarah Lynn) Nothnagel. "Development of a cold gas propulsion system for the TALARIS hopper". Accepted: 2011-11-18T19:30:10Z. Thesis. Massachusetts Institute of Technology, 2011. URL: <https://dspace.mit.edu/handle/1721.1/67069> (visited on 01/04/2022).
- [8] Babak Cohanim. "Mission design for safe traverse of planetary hoppers". Accepted: 2013-11-18T20:40:13Z. Thesis. Massachusetts Institute of Technology, 2013. URL: <https://dspace.mit.edu/handle/1721.1/82476> (visited on 09/28/2021).
- [9] Marian Daogaru et al. "Lunar Hopper Mk. II Enhancements Summary Report". original-date: 2017-02-09T17:04:01Z. PhD thesis. University of Southampton, 2016. 156 pp. URL: https://github.com/uoslunarhopper/phaseVIreport/blob/605b2e4b707eb2ceaea450d8b9a01efa60f15932/GDP_Report_Final.pdf (visited on 09/28/2021).
- [10] Gabriele Podestà. "Lunar Nano Drone for a mission of exploration of lava tubes on the Moon: Propulsion System - Master's degree Thesis". PhD thesis. Politecnico di Torino, 2020. 122 pp.
- [11] Tim Craine and Matt Atwell. *Intuitive Machines' Micro-Nova Lava Tube Access - Lunar Surface Innovation Consortium Extreme Access Focus Group Telecon*. Intuitive Machines, Aug. 8, 2021.
- [12] Intuitive Machines. *Intuitive Machines and NASA Finalize Contract for Extreme Lunar Mobility Spacecraft*. Intuitive Machines. July 21, 2021. URL: <https://www.intuitivemachines.com/post/intuitive-machines-and-nasa-finalize-contract-for-extreme-lunar-mobility-spacecraft> (visited on 01/04/2022).

- [13] Karin Valentine. *NASA funds hopper to explore lunar polar craters*. ASU News. July 21, 2021. URL: <https://news.asu.edu/20210720-nasa-funds-hopper-explore-lunar-polar-craters> (visited on 01/04/2022).
- [14] National Aeronautics and Space Administration (NASA). *Exploration Systems Mission Directorate (ESMD) Course Material: Fundamentals of Lunar and Systems Engineering for Senior Project Teams, with Application to a Lunar Excavator*. Lunar Engineering Handbook. URL: <https://www.eng.auburn.edu/~dbeale/ESMDCourse/index.htm> (visited on 01/04/2022).
- [15] Jeremi Gancet et al. "LUVMI AND LUVMI-X: LUNAR VOLATILES MOBILE INSTRUMENTATION CONCEPT AND EXTENSION". In: (), p. 8.
- [16] Lunar and Planetary Institute. *Lunar South Pole Atlas*. 2022. URL: <https://www.lpi.usra.edu/lunar/lunar-south-pole-atlas/>.
- [17] Soderman. *Scale of Lunar South Polar Mountains*. Solar System Exploration Research Virtual Institute. URL: <https://sservi.nasa.gov/articles/scale-of-lunar-south-polar-mountains/> (visited on 01/04/2022).
- [18] *Lunar Reconnaissance Orbiter*. In: *Wikipedia*. Page Version ID: 1062501347. Dec. 28, 2021. URL: https://en.wikipedia.org/w/index.php?title=Lunar_Reconnaissance_Orbiter&oldid=1062501347 (visited on 01/03/2022).
- [19] Megan Henriksen. *Casting Light on Permanently Shadowed Regions | Lunar Reconnaissance Orbiter Camera*. Jan. 27, 2018. URL: <http://lroc.sese.asu.edu/posts/979> (visited on 01/03/2022).
- [20] Rick Chen. *VIPER*. National Aeronautics and Space Administration (NASA). Jan. 9, 2020. URL: <http://www.nasa.gov/viper> (visited on 09/25/2021).
- [21] *ESA EL3: Ideas for exploring the Moon with a European lander – CRISP*. Centro Ricerche Innovative per lo Spazio (CRISP). 2020. URL: <https://crisp.unipg.it/2020/05/esa-el3-ideas-for-exploring-the-moon-with-a-european-lander/> (visited on 01/01/2022).
- [22] European Space Agency. *European Large Logistics Lander*. URL: https://www.esa.int/Science_Exploration/Human_and_Robotic_Exploration/Exploration/European_Large_Logistics_Lander (visited on 01/04/2022).
- [23] National Aeronautics and Space Administration (NASA). *State-of-the-Art Small Spacecraft Technology Report - Small Spacecraft Systems Virtual Institute, Ames Research Center*. Moffett Field, California: Small Spacecraft Systems Virtual Institute, Ames Research Center, 2021. URL: <https://www.nasa.gov/smallsat-institute/sst-soa>.
- [24] *Confidential reference*. available on request.
- [25] *Lidar - Wikipedia*. URL: <https://en.wikipedia.org/wiki/Lidar> (visited on 01/06/2022).

-
- [26] V. Mitev et al. “Evaluation of novel technologies for the miniaturization of flash imaging lidar”. In: *International Conference on Space Optics — ICSO 2014*. International Conference on Space Optics — ICSO 2014. Vol. 10563. SPIE, Nov. 17, 2017, pp. 1437–1445. DOI: [10.1117/12.2304074](https://doi.org/10.1117/12.2304074). URL: <https://www.spiedigitallibrary.org/conference-proceedings-of-spie/10563/105634Z/Evaluation-of-novel-technologies-for-the-miniaturization-of-flash-imaging/10.1117/12.2304074.full> (visited on 10/22/2021).
- [27] Alexandre Pollini. “SPAD for space active debris removal and exploration LiDARs - International SPAD Sensor Workshop”. June 5, 2020. URL: https://www.imagesensors.org/Past%20Workshops/2020%20ISSW/Alexandre_Pollini_ISSW2020_CSEM.pdf.
- [28] Alexandre Pollini, Christophe Pache, and Jacques Haesler. “CSEM Space Lidars for Imaging and Ranging”. In: *IGARSS 2018 - 2018 IEEE International Geoscience and Remote Sensing Symposium*. IGARSS 2018 - 2018 IEEE International Geoscience and Remote Sensing Symposium. ISSN: 2153-7003. July 2018, pp. 1849–1852. DOI: [10.1109/IGARSS.2018.8519241](https://doi.org/10.1109/IGARSS.2018.8519241).
- [29] Georgios D. Tzeremes et al. “Altimetry, Imaging and Landing Location Selection Lidars for ESA Space Applications”. In: *IGARSS 2019 - 2019 IEEE International Geoscience and Remote Sensing Symposium*. IGARSS 2019 - 2019 IEEE International Geoscience and Remote Sensing Symposium. ISSN: 2153-7003. July 2019, pp. 4775–4778. DOI: [10.1109/IGARSS.2019.8900519](https://doi.org/10.1109/IGARSS.2019.8900519).
- [30] ECAPS by Bradford. *Bradford ECAPS - Products - 22N*. 2022. URL: <https://www.ecaps.space/products-22n.php> (visited on 01/03/2022).
- [31] Wiley J. Larson and J.R. Wertz. *Space Mission Analysis and Design*. 1st ed. Space Technology Library. Springer Netherlands, 1991. 813 pp. ISBN: 978-0-7923-0970-3. URL: <https://link.springer.com/book/9780792309710> (visited on 01/04/2022).
- [32] George P. Sutton and Oscar Biblarz. *Rocket Propulsion Elements, 9th Edition* | Wiley. Wiley.com. URL: <https://www.wiley.com/en-us/Rocket+Propulsion+Elements%2C+9th+Edition-p-9781118753651> (visited on 01/04/2022).
- [33] Ezgi Civek, Başar Seçkin, and Tuğrul Tınaztepe. “An Industrialization Model for Satellite Propulsion System Manufacturing, Assembly, Integration & Test”. In: June 12, 2009.
- [34] ESA Earth Observation Portal (eoPortal). *GPIM (Green Propellant Infusion Mission) / STP-2*. eoPortal Directory / Satellite Missions. 2022. URL: <https://directory.eoportal.org/web/eoportal/satellite-missions/g/gpim#lqy2M112bHerb> (visited on 12/27/2021).
- [35] Saft. *Saft Batteries MP 144350 xlr - Rechargeable Li-ion cell Datasheet*. 2018. URL: <https://go.epfl.ch/saftbattery>.
- [36] *Spacecraft Propellant Tanks - MT AEROSPACE*. URL: <https://www.mt-aerospace.de/files/mta/tankkatalog/MT-Tankkatalog.pdf>.
- [37] *SDL Thermal Straps*. Space Dynamics Laboratory (Utah State University). 2022. URL: <https://www.sdl.usu.edu/capabilities/science-engineering/thermal-management/thermal-straps> (visited on 12/29/2021).
-

- [38] Phong Nguyen et al. "Remote Marker-Based Tracking for UAV Landing Using Visible-Light Camera Sensor". In: *Sensors* 17 (Aug. 30, 2017), p. 1987. DOI: [10.3390/s17091987](https://doi.org/10.3390/s17091987).
- [39] Pär-Olof Johannesson. *What's the Difference Between Frame- and Event-Based LiDAR?* Electronic Design. Jan. 2021. URL: <https://www.electronicdesign.com/markets/automotive/article/21152870/terranel-what-s-the-difference-between-frame-and-eventbased-lidar> (visited on 01/04/2022).
- [40] Vanessa Mazzari. *What is LiDAR technology?* Génération Robots - Blog. Aug. 8, 2019. URL: <https://www.generationrobots.com/blog/en/what-is-lidar-technology/> (visited on 01/04/2022).
- [41] Mike Ball. *Long-Range High Scan Rate LiDAR for UAVs Introduced*. Unmanned Systems Technology. Apr. 30, 2019. URL: <https://www.unmannedsystemstechnology.com/2019/04/long-range-high-scan-rate-lidar-for-uavs-introduced/> (visited on 12/29/2021).
- [42] LS LiDAR. *HS Series High Speed LiDAR Scanner Products*. LS LiDAR. 2022. URL: <https://www.leishenlidar.com/lidar-sensor-products/high-speed-lidar-scanner-sensor/> (visited on 12/29/2021).

A Lidar calculations

In order to calculate requirements for the Lidar system, a minimum resolution needs to be set for a given sample rate. For instance, modern Lidar systems used in cars are usually set below the 100 Hz scan rate mark [39, 40], while recent systems for drones are capable of much higher frequencies such as 200 to 400 Hz [41, 42]. For the lunar reconnaissance drone, a sample rate of 300 Hz is estimated. The minimum resolution is fixed at 10 cm. This is based on the estimated wheel size of a typical lunar rover (around 50 cm) and the resolution to be set below this value. The maximum horizontal velocity of the drone can then be calculated with:

$$v_{hor,max} = f_{sample} \cdot resolution = 300 \text{ Hz} \cdot 0.1 \text{ m} = 30 \text{ m/s} \quad (1)$$

This value appears to be a reasonable maximum velocity for the drone. In addition, a flight altitude of 50 m is selected to stay within typical Lidar capabilities.

The resolution of the Lidar will be determined by the desired field of view (width of the terrain being mapped under the drone). This field of view and therefore the resolution of the Lidar have not been defined in this preliminary design project.

B Propulsion and flight trajectory calculations

B.1 Thrusters arrangement

Several potential placements of the four thrusters can be thought of and are represented on [Figure B.1](#).

Advantages and disadvantages of each option are briefly listed in [Table B.1](#). For option a), the torque required for a slewing movement of 45 ° is calculated [31] based on the preliminary flight simulation presented below ([subsection B.3](#)) and compared to available Reaction Wheels (RW) and Control Moment Gyroscopes (CMG) on the market. It can be concluded that RWs/CMGs are not suitable for the lunar reconnaissance drone, since these systems are too heavy as the required torque is too important.

It is decided to select option c) for the thruster arrangement of the drone, as it mitigates dust generation the best and allows for simple placement of the Lidar system and other sensors. In addition, quadcopter drone technology used on Earth can be used as reference for the control algorithms. The possibly higher propellant consumption is put up for these advantages.

B.2 Flight simulation assumptions

Assumptions made for all calculations are the following:

- The drone's mass is constant and fixed at 15 kg.
- The drone's change in mass during the flight does not influence the propellant consumption.

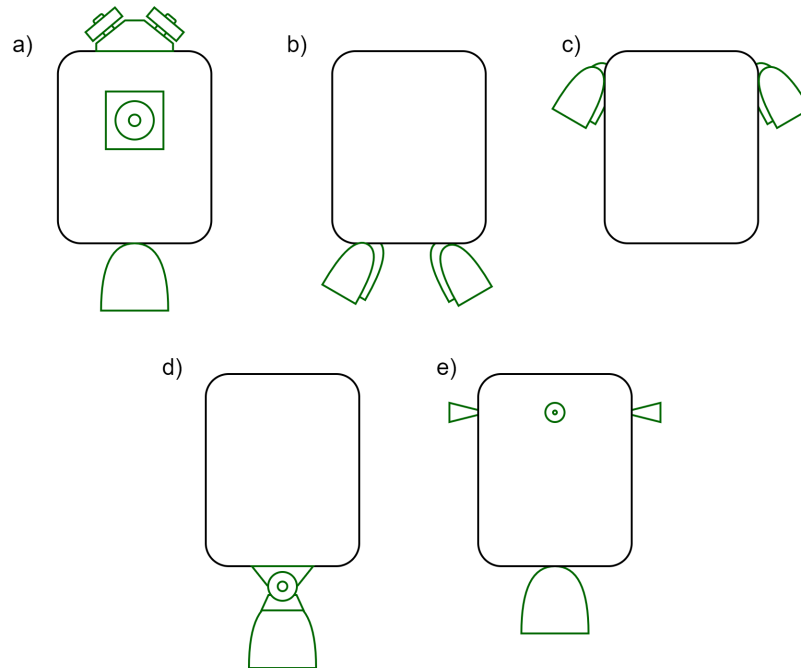


Figure B.1: Possible thrusters arrangements: a) One single thruster with reaction wheels / control moment gyroscopes b) 3-4 thrusters on the bottom c) 3-4 lateral thrusters d) One single thruster on gimbal e) One single thruster and 3-4 small lateral thrusters.

- The lunar gravity constant is 1.62 m/s^2 .
- Flight trajectories are two-dimensional.
- Horizontal flight velocities should not exceed 30 m/s .

From the initial mass of 15 kg of the drone and the lunar gravity, a minimum take-off thrust of 26.5 N is required. This is a first constraint on the thruster system.

B.3 Preliminary simulations

In a next step, three different flight profiles are simulated using Simulink: A one-way ballistic flight of around 400 m of distance and 120 m maximum altitude, a hovering flight with purely vertical and horizontal displacements (400 m horizontal distance and 50 m flight altitude) and a combined flight with ballistic take-off and landing and intermediate horizontal flight. The individual thrusts are manually inserted and resolution limited by the functions blocks of Simulink. For this reason, the flight trajectories are not perfectly symmetric on the plots (Figure B.2) below.

From the average thrust forces F , the thrust durations t_F and the specific impulse I_{sp} set at 240 s , the required propellant mass can be calculated for each case with:

$$m_{prop,required} = \frac{F \cdot t_F}{g_0 \cdot I_{sp}} \quad (2)$$

Table B.1: Thruster arrangement advantages and disadvantages

Option	Advantages	Disadvantages
a)	+ One thruster only + Precise navigation	- High power consumption - High overall mass - RW / CMG volume - Orientation speed limited by drone mass - Dust generation - Lidar placement
b)	+ Simple control + Reliable	- Weight - Dust generation - Lidar placement limited - Higher propellant consumption
c)	+ Less dust generation + Lidar placement	- Higher propellant consumption
d)	+ Simple control	- Moving mechanism - High risk - Dust generation - High volume and mass - Development time - Landing feet
e)	+ Simple control + Precision + Reliable	- Dust generation - Higher propellant consumption - Lidar placement - Landing feet

This yields the results presented in [Table B.2](#). Since a constant flight altitude and relatively low flight velocities are of preference for the mapping of the ground, the ballistic trajectory can be directly discarded. In addition, the combined flight does not yield many advantages over the "hovering" flight, besides the slightly smaller propellant required. It is hence decided that the hovering profile is the most advantageous one and the one to be selected for the mission. For reasons of completeness, a more precise flight analysis of the hovering flight profile is realized in a next step.

Table B.2: Results of preliminary trajectory calculations

Flight profile	Average thrust [N]	Total thrust duration [s]	Required propellant mass [kg]
Ballistic	35	6	0.089
Hovering	19.125	16	0.13
Combined	22.76	10.2	0.099

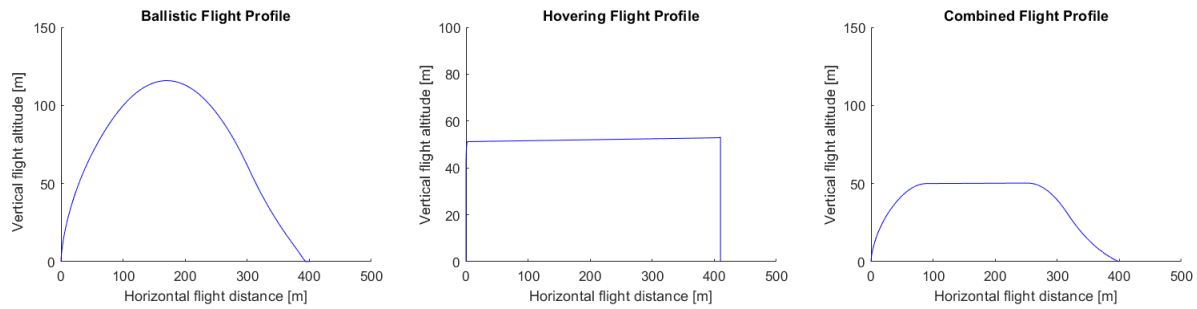


Figure B.2: Three different flight profiles analyzed.

B.4 Detailed flight simulation

In this more realistic flight simulation (again realized in Simulink), a trajectory closer to the final ConOps is analyzed: Vertical take-off thrust until the desired flight altitude, initial horizontal thrust and hovering thrust for 400 m, horizontal thrust in opposite direction and hovering back the 400 m, hovering thrust plus breaking thrust and finally descent thrust. This flight profile is simulated once with simplified thrusters angled in horizontal and vertical directions, and once with four thrusters at 45°. The results of these simulations are presented in table [Table B.3](#).

Table B.3: Results of the more detailed simulation

Flight profile	Total impulse [Ns]	Required propellant mass [kg]
Hovering, horizontal & vertical thrusters	2151	0.089
Hovering, thrusters angled at 45°	19.125	0.13

Two major aspects stand out from these results: Firstly, the total propellant required is significantly higher in the more detailed calculations than in the preliminary ones. Secondly, the flight with thrusters angled at 45° logically requires more propellant than the simplified first one.

B.5 More detailed flight simulation

Finally a third even more detailed version of the flight simulation is realized, where each angled thruster is individually simulated. The Simulink layout for this version is presented on [Figure B.4](#) below.

On [Figure B.3](#), the drone's decrease in mass due to propellant consumption is presented. From an initial mass of 15 kg, the drone returns with a final mass of around 14 kg, resulting in 1 kg of propellant required for one flight of around 800 m of total horizontal flight distance and 50 m of ascent and descent and total flight time of 65 s. For the rest of the mission, a factor of two is introduced in the propellant required, resulting in a comfortable margin. Also, a horizontal flight distance of 1000 m is considered, as thruster angles are not optimized and drone mass loss is not considered so far.

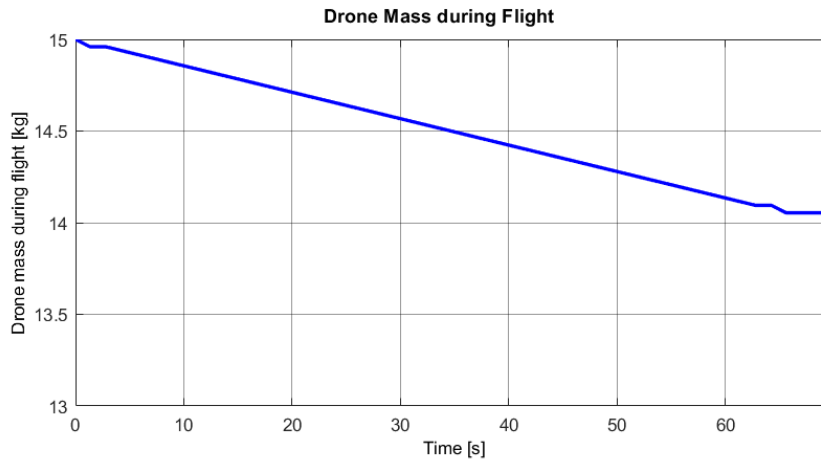


Figure B.3: Drone mass decrease due to propellant consumption.

B.6 Propellant tank mass estimation

The calculations for the propellant tank is based on the estimating calculations proposed in the handbook by Larson et al [31]. The material selected is Titanium for its low coefficient of thermal expansion and the shape of the tank is spherical. The assumptions and parameters used for these calculations are:

- Propellant density (LMP-103S): 1240 kg/m^3
- Titanium max. allowable stress: 825 Mpa
- Titanium density: 4400 kg/m^3
- Max. expected operating pressure P_p : 2.4 MPa
- Perfect gas law is considered
- Conservation of energy is considered

Using a Factor of Safety (FoS) of two, a tank wall thickness of 0.21 mm is found. In the following, a more realistic thickness of 1.5 mm is used instead. A propellant tank weight of 0.074 kg can be calculated (including an additional 20% margin).

B.7 Pressurant mass and tank mass estimation

For the calculation of the pressurant mass and tank mass, the procedure proposed by Sutton et al. in *Rocket Propulsion Elements* is followed using the following parameters:

- Ambient temperature of $T_0 = 275 \text{ K}$

- Same propellant and tank material properties as in [subsection B.6](#)
- Ideal flow conditions and an adiabatic process are considered
- Initial storage pressure $P_0 = 14$ MPa
- Final tank pressure $P_p = 2.4$ MPa

Two different pressurants are compared: Nitrogen and Helium. The results are shown in [Table B.4](#). The latter yields a lighter tank after calculations: 0.045 kg (20% margin included) of mass, with a wall thickness of 0.6 mm and a FoS of two.

Table B.4: Pressurant comparison

Pressurant	Nitrogen	Helium
Tank radius [m]	0.0673	0.0344
Tank wall thickness [mm]	1	0.6
Tank mass [kg] (incl. 20% margin)	0.338	0.045

B.8 Limitations

The simulations realized for this project yield several limitations, namely:

- The drone's mass is considered to be constant at all time. In reality, this changes with the propellant consumption and must be included in future studies.
- The propellant consumption is based on simplified equations and do not consider any losses or other details. The resulting values need therefor to be taken with caution. A more detailed simulation using exact consumption parameters provided by the thruster manufacturer would be the next step to do.
- The Simulink model is hard coded by hand and values visually adapted in order to obtain "realistic" flight profiles. A more detailed and preciser model (implying longer calculation times) is required for better estimation of the drone's flight behaviour.
- For the propellant and pressurant tank calculations, a more in-depth approach is needed, as some of the results do not appear to be reasonable (e.g. pressurant tank wall thickness of 0.6 mm). Also, available tank dimensions on the market need to be included in the study.
- The thruster angles are set at 45° in the simulations, resulting in significant thrust losses in the horizontal direction. A optimal balance between thruster angle and dust generation has to be found in the future.

Nevertheless, the results given by the different simulations provide a useful reference point, not least since very pessimistic assumptions and worst-case values are used. In reality, less propellant consumption can probably be expected.

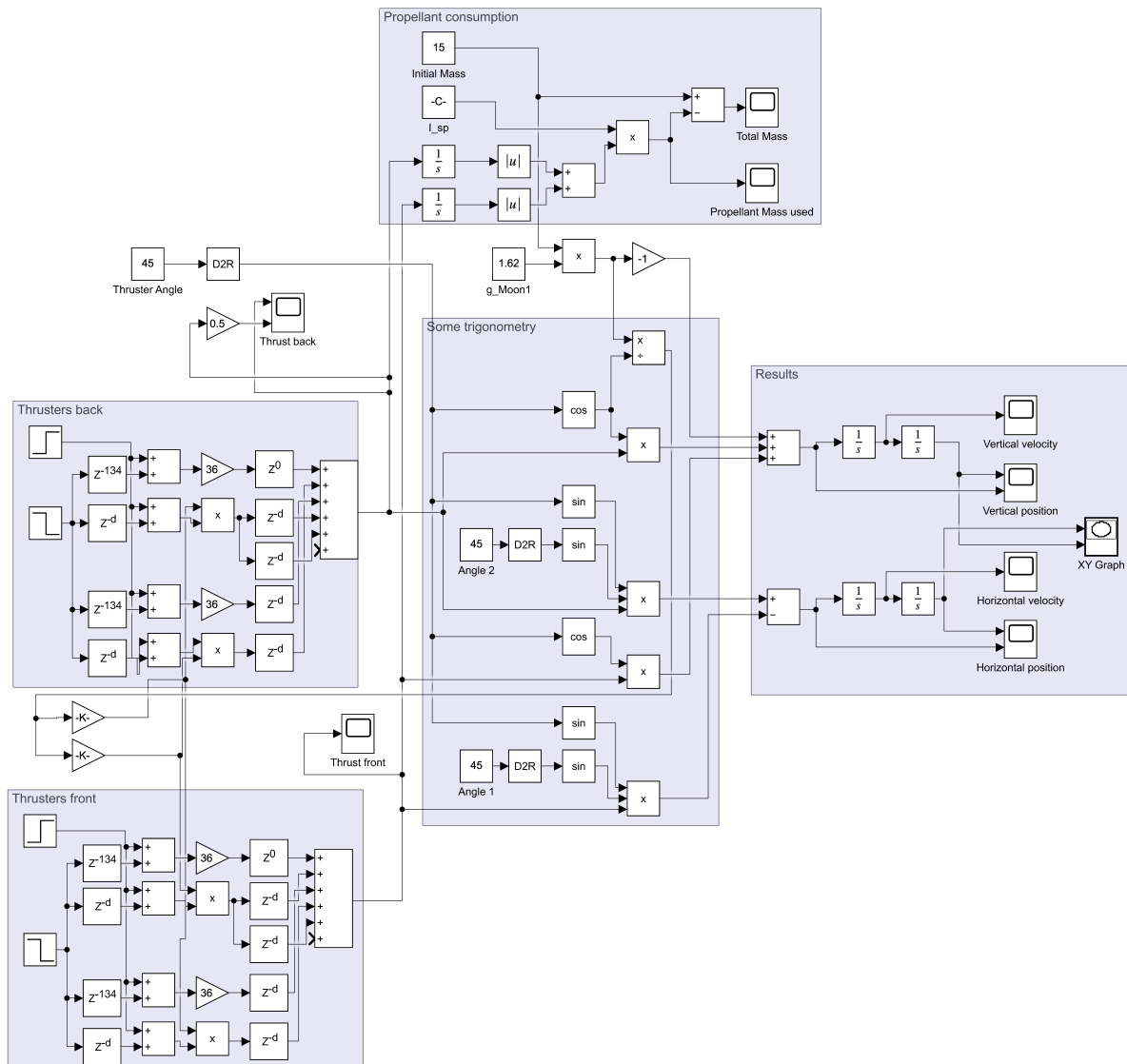


Figure B.4: Detailed flight profile simulation in Simulink.

C Thermal analysis

The evolution of the drone's temperature with respect to time is performed by calculating the heat transfer rate and by using a discrete time step model.

C.1 Assumptions

The assumptions for this model are:

- The drone is thermally independent of the rover (during the flight).
- The drone has a uniform temperature.
- The drone has a mass of $m = 15$ kg and an average heat capacity of $c_p = 900$ J/K (mix of common spacecraft materials).
- The drone's initial temperature is supposed to be $T = 5$ °C.
- The drone's surface is approximated as a cylinder of height $h = 0.4$ m and radius $r = 0.25$ m. It has a surface area of $A = 1.021$ m².
- Heat is only transferred to the environment by radiation.
- All the incoming and internally generated heat is considered as a single heat source term \dot{Q}_{gen} [W]. This heat is produced by:
 - Exposure to sunlight
 - Joule heating of the electronic components¹.
 - Heating due to the thrusters firing.
- The background black body radiation is estimated at to be emitted at $T_\infty = 4$ K, which is equal to the black body temperature of deep space.
- The drone is considered as a grey body with its emissivity and absorptivity being equal and independent of the wave length: $\epsilon_\lambda = \epsilon = \alpha = \alpha_\lambda$.

C.2 Calculations

The transferred by radiation \dot{Q}_{rad} [W] is given by:

$$\dot{Q}_{rad} = \dot{Q}_{abs} - \dot{Q}_{emi} \quad (3)$$

with \dot{Q}_{emi} [W] and \dot{Q}_{abs} [W] the emitted and absorbed heat respectively, which are equal to:

$$\dot{Q}_{emi} = -\sigma \cdot \epsilon \cdot A \cdot T^4 \quad (4)$$

$$\dot{Q}_{abs} = \sigma \cdot \epsilon \cdot A \cdot T_\infty^4 \quad (5)$$

where σ is the Stephan-Boltzmann constant. The temperature difference dT [K] between each time step dt [s] is then given by:

¹Approximately equal to the total electric power of the drone.

$$dT = \frac{\dot{Q}_{rad} + \dot{Q}_{gen}}{m \cdot c_p} \cdot dt \quad (6)$$

C.3 Temperature change results

The temperature change with respect to time, thermal source power and emissivity/absorptivity can be seen in [Figure C.1](#). A detailed time evolution for $\dot{Q}_{gen} = 400 \text{ W}$ and $\epsilon = \alpha = 0.8$, which is representative of white paint, is shown in [Figure C.2](#). The temperature of the drone after a very long time (equilibrium temperature) is shown in [Figure C.3](#).

These results clearly show that without installing radiators, the generated heat is not well evacuated. To avoid this added complexity, the internal heat source due to the electric power consumption and due to the thrusters firing should be limited to around 500 W. The surface finish (coatings and paints) can be chosen accordingly to limit the temperature change during a mission. If the drone should be able to function in the sunlight, a surface with a high ratio of emissivity over absorptivity ϵ/α should be chosen.

It is also important to note that if the drone is not heated, its temperature will drop rapidly as seen in [Figure C.4](#). The drone should therefore rapidly be protected under an insulating cover with low emissivity when not in use.

C.4 Model limitations

The thermal evolution model used here presents multiple limitations which should be studied in future developments. Ideas of further studies are listed here:

- Modeling the temperature distribution in the drone with local hot and cold spots for different scenarios.
- Effect of the sunlight in more detail:
 - Illumination on one side of the drone only.
 - Sunlight for only a part of the flight / of the missions.
- Optimizing the surface coating for emissivity ϵ and absorptivity α separately, as well as their ratio.

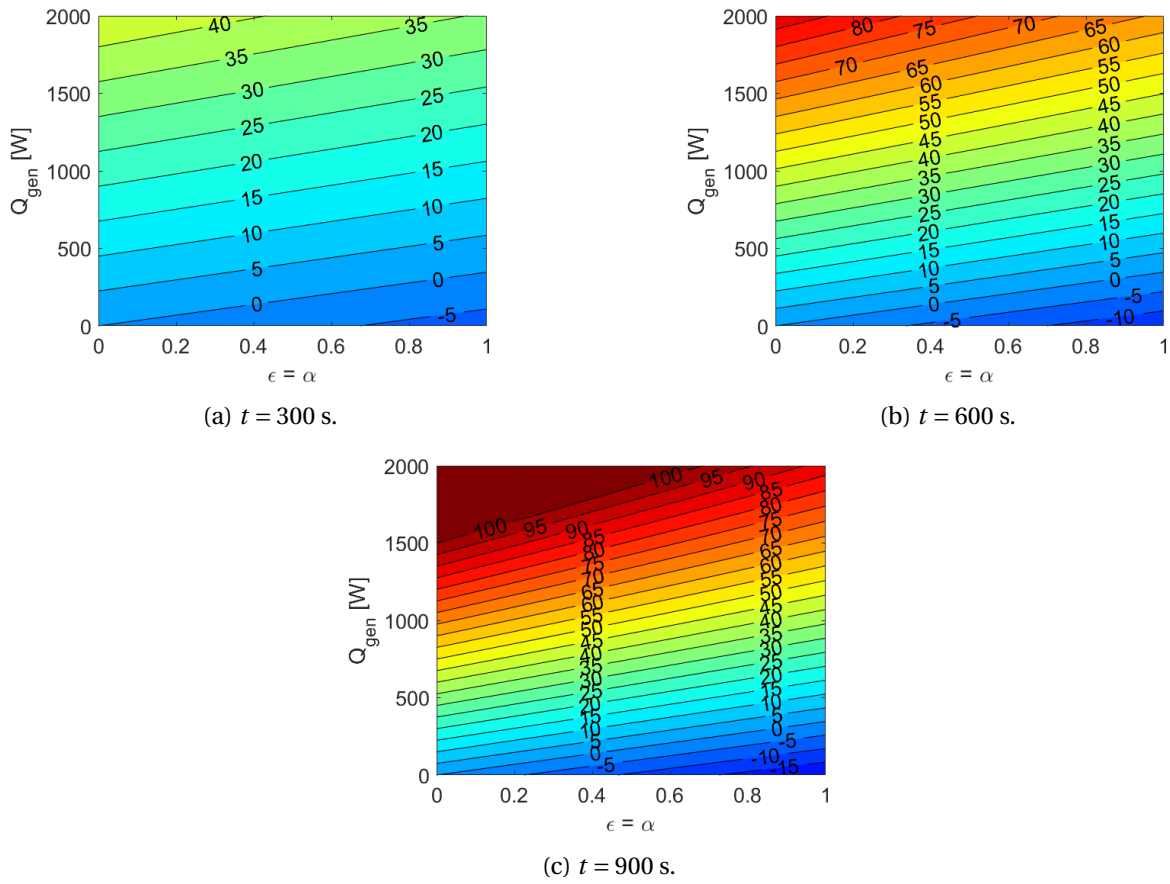


Figure C.1: Drone temperature change ΔT [K] for various elapsed times t with respect to the thermal source power \dot{Q}_{gen} and the emissivity/absorptivity $\epsilon = \alpha$.

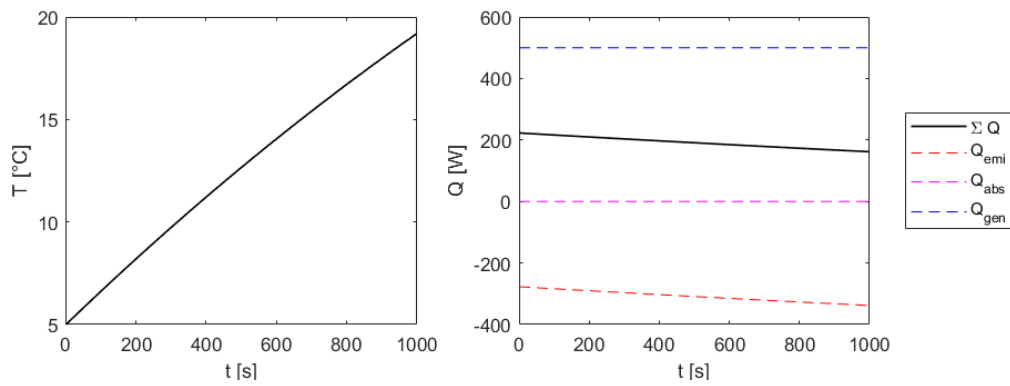


Figure C.2: Evolution of the drone temperature T with respect to time t for $\dot{Q}_{gen} = 500$ W and $\epsilon = \alpha = 0.8$.

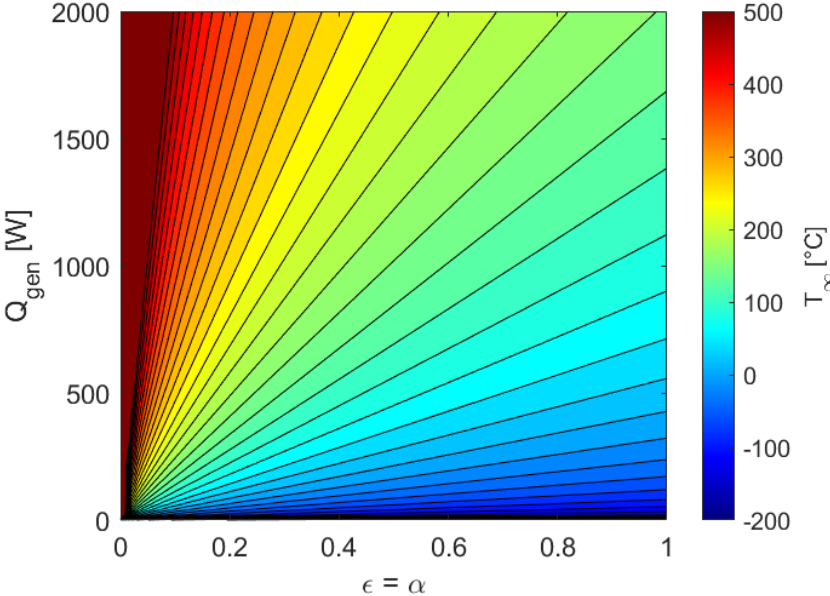


Figure C.3: Drone equilibrium temperature T_{∞} with respect to the thermal source power Q_{gen} and the emissivity/absorbtivity $\epsilon = \alpha$.

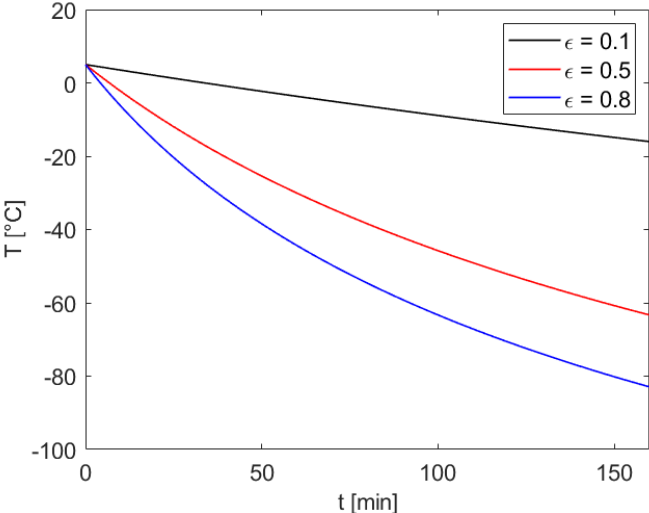


Figure C.4: Drop of the drone temperature T with respect to time t , when the thermal source power is zero.

D Power calculations

With a preliminary power consumption P_e estimated at 429 W (see 8.2.2) and a flight or operational time t_{op} of estimated 10 minutes, the required battery capacity C_r can be calculated:

$$C_r = \frac{P_e \cdot t_{op}}{60 \cdot DoD \cdot N \cdot n} = 55.9 \text{Wh} = 2 \text{Ah} \quad (7)$$

for a bus voltage of 28 V, where DoD is the Depth-of-Discharge of 0.2, N is the selected amount of batteries (eight) and n is the battery-to-load transmission efficiency set at 0.8 [31]. The amount of batteries can be determined from the bus voltage to be used for a given battery capacity:

$$N = \left\lceil \frac{U_{bus}}{C_r} \right\rceil \quad (8)$$

The light-weight *MP 144350 xlr Rechargeable Li-ion cells* by Saft (Figure D.1) are suitable for this mission and have the following specifications (Table D.1):

Table D.1: MP 144350 xlr Rechargeable Li-ion cell specifications [35]

Battery	Saft MP 144350 xlr
Form factor	Prismatic
Nominal voltage	3.65 V
Nominal capacity	2.6 Ah
Max. cont. discharge current	5.0 A
Max. pulse discharge rate	10.0 A
Cycle life	1100
Typical weight	66 g
Discharge temp. range	-35 to 60 °C
Charge temp. range	-30 to 60 °C

With the selected batteries by Saft, a total battery mass of 0.8 kg and a total capacity of 20.8 Ah is calculated, resulting in a theoretical operational (flight) time of 13 minutes.

E Risk Analysis

A preliminary Failure Mode and Effects Analysis (FMEA) is presented in table Table E.1. Note that this analysis needs to be revisited and updated while developing and planning the mission. The version presented here may be incomplete and requires further elaboration in the future.

Table E.1: Preliminary risk analysis

Component name	Function	Potential failure mode	Potential cause(s) /mechanism	Mission phase	Local failure effect	Global failure effect	Probability (P)	Severity (S)	Risk level	Mitigation / Requirements
Thrusters	Provide thrust to the drone for flight	One thruster does not operate correctly	Internal thruster issue	Flight	Thruster does not provide required thrust	Drone cannot fly nominally	2	4	5	Develop and test a emergency flight mode using only three thrusters, fire tests before flight
		Two or more thrusters do not operate	Internal thruster issue	Flight	Thrusters does not provide required thrust	Drone cannot fly at all	1	5	5	Extensive testing of thrusters before mission, fire tests before flight
Tanks	Store propellant/pressurant for the propulsion system	Pressurant tank does not work nominally	Leakage in the tank or problematic temperature of the pressurant	Flight + fueling	Pressurant cannot maintain pressure in propellant tank	Drone's flight performance decreases over time	1	3	2	Testing before mission, "reduced thrust" flight mode, fire tests before flight
		Propellant tank does not work nominally	Leakage in the tank or problematic temperature of the propellant	Flight + fueling	Thrusters do not receive sufficient propellant	Drone's flight performance is limited	1	4	3	Testing before mission, fire tests before flight
Pressure regulator	Regulates pressurant pressure flowing into propellant tank	Pressure regulator does not operate correctly	Valve gets blocked, not enough power to actuate the valve	Flight	Pressurant pressure is not nominal	Drone's flight performance decreases over time	1	3	2	Testing before mission, "reduced thrust" flight mode
Valves	Regulate pressurant/propellant flow rate in the propulsion system	Pressurant fill/drain valves do not operate correctly	Valve gets blocked, not enough power to actuate the valve	Fueling	Pressurant tank cannot be refueled	Drone's flight performance decreases over time	1	3	2	Testing before mission, "reduced thrust" flight mode
		Propellant fill/drain valves do not operate correctly	Valve gets blocked, not enough power to actuate the valve	Fueling	Propellant tank cannot be refueled	Drone cannot fly multiple times	1	4	3	Testing before mission, power supply redundancy
		Thruster valves do not operate correctly	Valve gets blocked, not enough power to actuate the valve	Flight	Propellant inflow into thrusters is limited	Drone's flight performance is limited	1	4	3	Testing before mission, power supply redundancy
Fuel lines	Provide physical distribution of pressurant/propellant	Fuel lines do not / partly distribute pressurant/propellant	Leakage	Flight	Pressurant and/or propellant is not correctly distributed	Drone's flight performance is limited	1	4	3	Testing before mission, "reduced thrust" flight mode
IMUs	Provide gyro and accelerometers measurements for navigation purposes	IMUs provide wrong data or fail	Wrong calibration, damaged or faulty electronics	Flight	Wrong or corrupted navigation data	Drone's flight performance is reduced	2	4	5	IMU calibration and testing, cross-checking with 3D mapping data
Range finder	Measures drone altitude above ground	Provides wrong data or fails	Wrong calibration, damaged or faulty electronics, dust on optics	Flight	Wrong altitude or no data is measured	Drone's flight performance is reduced	1	3	2	Testing, cross-checking with optical tracking sensors
Optical camera	Tracks lights on drone base for take-off and landing	Does not manage to track the base	Faulty tracking lights, dust on optics	Flight	Drone cannot track base for take-off or landing	Drone flight performance constrained	2	4	5	Testing, cross-checking with range finder
Lidar system	Scans and 3D maps lunar ground; provides data to drone navigation	Scanning fails	Dust on optics, lidar system faulty	Flight	Ground cannot be mapped	Drone cannot navigate correctly, data not available for rover mission	2	5	8	Extensive testing before mission, flame deflector to reduce dust dispersion
Batteries	Provide power to all drone subsystems	Batteries do not operate correctly	Temperature not suitable, cables disconnected	Flight	Power is not guaranteed	Drone cannot operate	1	5	5	Redundant batteries and testing
Antenna	Transmits/receives data/commands to/from the drone base	Communication between base and drone fails	Drone out-of-sight, defect antenna	Flight	Housekeeping data cannot be sent to base, commands cannot be received	Drone flight performance reduced, limited mission flexibility	1	3	2	Testing, data transmission via cable once landed

OBC	Processes and handles data in the avionics and CDH subsystems	OBC fails or operates at reduced performance	Radiation or other damage, temperature not suitable	All	Crucial data processing in drone not realized	Drone cannot operate	1	5	5	Radiation hardened hardware, cross-checking software and redundancy
Data storage medium	Temporarily stores data (3D mapping data, etc.)	Data cannot be stored or gets corrupted	Radiation or mechanical damage of storage medium	Flight	3D mapping data not available or corrupted	Data not available for rover mission	1	4	3	Redundant storage
Power interface	Connects drone to rover power system for recharging	Drone cannot be connected	Mechanical failure of connection mechanism	Standby	Power cannot be transmitted to drone	Drone cannot be recharged and fly again	2	4	5	Testing of connection mechanism, solar panels on drone
Propellant interface	Connects drone to base tanks for refueling	Drone cannot be connected	Mechanical failure of connection mechanism	Standby	Pressurant and propellant cannot be refuel	Drone cannot be refueled and fly again	2	4	5	Testing of connection mechanism
Signal interface	Connects drone to rover for 3D mapping data transmission	Drone cannot be connected	Mechanical failure of connection mechanism	Standby	Data via cable does not work	3D mapping data cannot be transmitted to rover	2	4	5	Wireless (slower) data transmission, testing of connection mechanism
Radiation cover	Protects drone from radiation when in stand-by mode	Cover does not open	Mechanical failure of cover actuation	Standby	Drone cannot be released	Mission cannot be executed	1	5	5	Testing of mechanism
		Cover does not close	Mechanical failure of cover actuation	Standby	Drone is not protected from radiation	Long-term radiation damage of the drone's electronics and reduced mission performance	1	3	2	Radhard hardware, testing of mechanism
Tracking lights	Provide tracking points for drone's optical camera system	Tracking lights do not work	Mechanical/thermal damage, dust on lights	Flight	Light cannot be used by drones optical sensors	Drone flight performance constrained	1	4	3	Testing, reduce dust dispersion
Hold-down mech.	Holds drone to base when not in flight phase	Hold-down mech. does not release	Mechanical failure	Standby	Drone cannot be released	Mission cannot be executed	1	5	5	Testing of mechanism
		Hold-down mech. does not hold down	Mechanical failure	Standby	Drone cannot be secured to base	Drone can be damaged during standby or transport phase	1	4	3	Testing of mechanism
Heaters	Keep drone in operations temperature range	Heaters do not work nominally	Power issue, faulty thermal measurements	All	Temperature exceeds operational or survival temp. ranges of components	Limited or failed drone performance	1	5	5	Testing of thermal system
Heat straps	Provide internal heat distribution via conduction	Heat is not distributed correctly	Straps disconnected due to mechanical damage	All	Heat cannot be dissipated in the system	Limited or failed drone performance	1	5	5	Use adequate mounting/assembly techniques



Figure D.1: MP 144350 xlr Rechargeable Li-ion cell by Saft [35].

F Illustrations

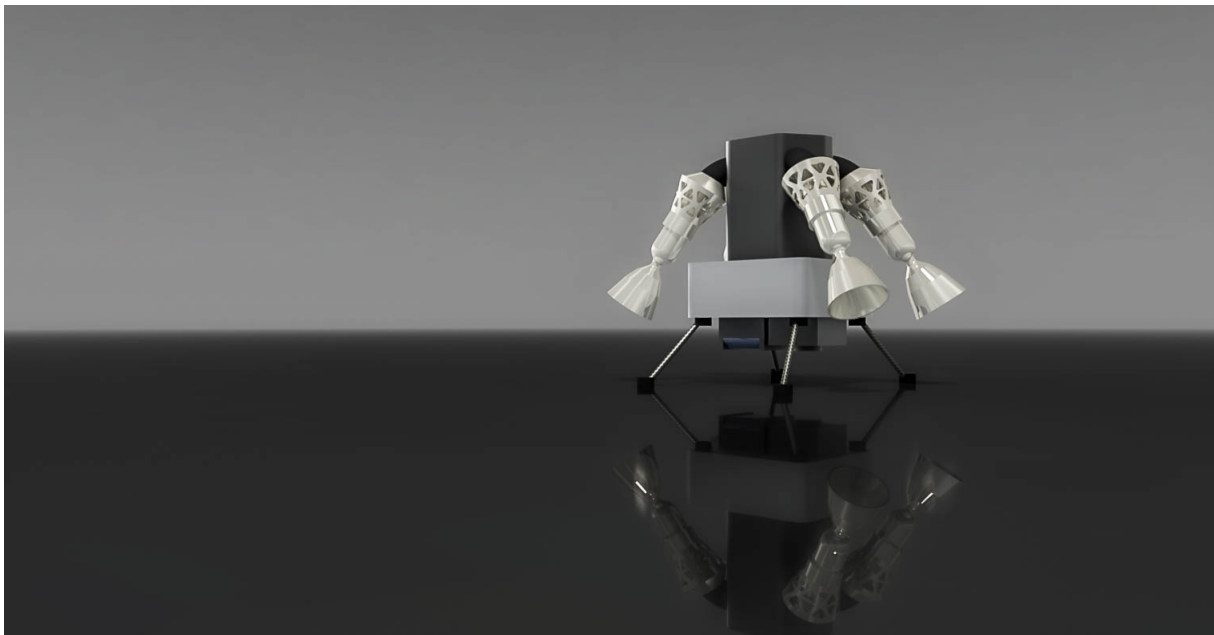


Figure F.1: CAD render of the lunar reconnaissance drone.



Figure F2: Illustration of the drone (Original image: NASA).



Figure F3: Illustration of the drone (Original image: NASA).